

**Dissertation zur Erlangung des Doktorgrades
der Fakultät für Chemie und Pharmazie
der Ludwig-Maximilians-Universität München**



**Anticancer effects and antimetastatic mechanisms
of novel indirubin derivatives**

Christine Ann Kressirer
(maiden name: Weber)

from Milwaukee, WI USA

2010

Erklärung:

Diese Dissertation wurde im Sinne von §13 Abs. 3 bzw. 4 der Promotionsordnung vom 29. Januar 1998 von Frau Prof. Dr. Angelika M. Vollmar betreut.

Ehrenwörtliche Versicherung

Diese Dissertation wurde selbstständig, ohne unerlaubte Hilfe erarbeitet.

München, den 14.06.2010

Christine Kressirer (geb. Weber)

Dissertation eingereicht am: 14.06.2010

1. Gutachter: Prof. Dr. rer. nat. Angelika Vollmar
2. Gutachter: Prof. Dr. rer. nat. Marianne Jochum

Mündliche Prüfung am: 13.07.2010

Dedicated to my family

The most exciting phrase to hear in science, the one that heralds new discoveries,
is not 'Eureka!' but 'That's funny...'

Isaac Asimov

CONTENT

CONTENT.....	I
INDEX OF FIGURES.....	V
INDEX OF TABLES.....	VI
ABBREVIATIONS.....	VII
1 INTRODUCTION.....	1
1.1 Background: New aspects of anticancer drug discovery.....	1
1.2 The role of natural products in treatment of diseases.....	3
1.3 Indirubins as anticancer compounds.....	4
1.3.1 History of indirubins.....	4
1.3.2 6BIO and 7BIO: Specific derivatives of indirubins.....	5
1.3.3 Kinase screening with indirubin derivates.....	7
1.4 Metastatic cancer: Treatments and targeted mechanisms.....	10
1.4.1 Standard treatments for metastatic cancer.....	11
1.4.2 Regulation and signaling of tumor cell migration.....	12
1.4.2.1 The actin cytoskeleton.....	14
1.4.2.2 Akt as a cellular key regulator.....	15
1.4.2.3 β 1 Integrin as a main mediator of cell migration.....	17
2 AIMS OF THE STUDY.....	20
a) Antitumor activities of 6BIO and 7BIO.....	20
b) Effects of 6BIO and 7BIO on metastatic pathways.....	20
c) Effects of 6BIO on migratory signaling targets.....	20
d) Effects of 6BIO in different cell models.....	20
3 MATERIALS AND METHODS.....	21
3.1 Materials.....	21
3.1.1 Study compounds: 6BIO and 7BIO.....	21
3.1.2 Biochemicals, inhibitors, dyes, and cell culture reagents.....	21
3.1.3 Technical equipment.....	22

3.2	Methods.....	23
3.2.1	Cell culture	23
3.2.1.1	Cell lines: Skbr3 and L3.6pl.....	23
3.2.1.2	Cultivation of cell lines	23
3.2.1.3	Freezing, thawing and long term storage	23
3.2.2	Flow cytometry	24
3.2.2.1	Apoptosis analysis.....	24
3.2.2.2	Anoikis analysis	25
3.2.2.3	Cell cycle analysis	25
3.2.2.4	β 1 Integrin surface expression	26
3.2.3	Cell viability measurements	26
3.2.4	Proliferation	26
3.2.5	Migration and invasion.....	27
3.2.5.1	Wound healing assay	27
3.2.5.2	Migration through membranes.....	27
3.2.5.3	Chemotaxis assay	28
3.2.5.4	Matrigel TM invasion assay	29
3.2.6	Cell adhesion on fibronectin	29
3.2.7	Western blot	29
3.2.7.1	Sample preparation	29
3.2.7.2	Immunoprecipitation	30
3.2.7.3	Protein quantification	30
3.2.7.4	SDS-PAGE.....	31
3.2.7.5	Tank blotting.....	31
3.2.7.6	Detection	32
3.2.7.7	Staining of gels and membranes.....	33
3.2.8	Confocal laser scanning microscopy (CSLM)	34
3.2.9	Skbr3 and fibroblast spheroids	34
3.2.9.1	Metabolic inhibition of Skbr3 spheroids	34
3.2.9.2	Skbr3 spheroid confrontation with fibroblast spheroids	35
3.2.10	Statistical analysis	35

4	RESULTS.....	36
4.1	Antitumor effects of 6BIO and 7BIO <i>in vitro</i>.....	36
4.1.1	Effects of 6BIO and 7BIO on apoptosis.....	36
4.1.2	Effects of 6BIO and 7BIO on anoikis induction.....	37
4.1.3	Effects on tumor cell proliferation by 6BIO and 7BIO treatment.....	38
4.1.4	Effects of 6BIO on cell viability in Skbr3 breast cancer cells.....	39
4.1.5	Breakdown of cell cycle upon 6BIO treatment.....	39
4.2	Different effects of 6BIO and 7BIO on metastatic pathways.....	41
4.2.1	Impairment of wound healing by 6BIO treatment.....	41
4.2.2	Effect of 6BIO on migration through Transwell™ inserts.....	42
4.2.3	Effects of 6BIO on Skbr3 chemotaxis in response to a FCS gradient.....	43
4.2.4	Effects of 6BIO on Skbr3 invasion through Matrigel™.....	44
4.2.5	Effect of 6BIO on tumor cell adhesion.....	44
4.3	β1 Integrin expression.....	46
4.3.1	β1 Integrin expression on the Skbr3 cell surface.....	46
4.3.2	Total β1 integrin expression of Skbr3 cells.....	47
4.4	Effects of 6BIO on migratory signaling pathways.....	49
4.4.1	Alteration of Akt expression following 6BIO treatment.....	49
4.4.2	Erk and FAK levels following 6BIO treatment.....	51
4.5	Actin cytoskeleton signaling upon 6BIO treatment.....	52
4.5.1	Effects on the actin cytoskeleton by 6BIO treatment.....	53
4.5.2	Expression of Rac upon 6BIO treatment.....	54
4.6	Effects of 6BIO 3D spheroids.....	55
4.6.1	Disruption of Skbr3 and fibroblast spheroids by 6BIO treatment.....	55
4.6.2	Disruption of Skbr3 spheroid invasion by 6BIO in a confrontation assay.....	57

5	DISCUSSION.....	58
5.1	Virtual comparison of 6BIO and 7BIO	58
5.2	Antitumor activities of 6BIO and 7BIO	59
5.3	Migration, invasion and adhesion after exposure to 6BIO or 7BIO	59
5.4	β1 Integrin and the actin cytoskeleton.....	60
5.5	Metastatic signaling targets.....	61
5.6	Effects of 6BIO on Skbr3 and fibroblast spheroids	63
6	SUMMARY	64
7	REFERENCES	67
8	APPENDIX.....	76
8.1	Publications.....	76
8.1.1	Original publications.....	76
8.1.2	Poster presentations	77
8.2	Grants and awards.....	77
8.3	Curriculum Vitae	78
8.4	Acknowledgments	79

INDEX OF FIGURES

Figure 1.1	2-D Structure of indirubin derivatives	6
Figure 1.2	Docking assay results	9
Figure 1.3	<i>In vitro</i> kinase assay results	10
Figure 1.4	Basic overview of metastatic signaling.....	12
Figure 1.5	Cell migration	13
Figure 1.6	Cell motility model.....	15
Figure 1.7	Model of Akt and Akt activation.....	16
Figure 1.8	Structure and activation of integrins.....	18
Figure 1.9	Integrin regulation and recycling	19
Figure 3.1	Chemotaxis assay in an IBIDI™ μ -slide	28
Figure 4.1	Induction of apoptosis by indirubin derivatives.....	36
Figure 4.2	Mild anoikis-inducing effects of 6BIO and 7BIO	37
Figure 4.3	Reduced proliferation by BIO's in a dose-dependent manner.....	38
Figure 4.4	Significant effect on cellular viability by treatment with 6BIO.....	39
Figure 4.5	Effect of 6BIO treatment on the cell cycle	40
Figure 4.6	Disruption of the wound closure ability by 6BIO	41
Figure 4.7	Reduction of the the tumor cell Transwell™ migration by 6BIO	42
Figure 4.8	Disruption of the directional cell migration by 6BIO.....	43
Figure 4.9	Disruption of the Skbr3 invasion through Matrigel™ by 6BIO	44
Figure 4.10	Adhesion of tumor cells to attractants	45
Figure 4.11	Surface β 1 integrin expression by 6BIO treatment.....	47
Figure 4.12	Expression of total β 1 integrin by 6BIO treatment.....	48
Figure 4.13	Total and active β 1 integrin after 6BIO treatment.....	48
Figure 4.14	Reduction of the activated form of Akt by 6BIO treatment.....	49
Figure 4.15	Reduction of active Akt localization to lamellipodia by 6BIO	50
Figure 4.16	Reduction of pS473Akt cycling by 6BIO treatment.....	50
Figure 4.17	Effect on pErk or pFAK/tot. FAK expression in Skbr3 cells by 6BIO ..	51
Figure 4.18	Effect of 6BIO treatment on FAK expression and distribution	52
Figure 4.19	Alteration of the actin cytoskeleton upon 6BIO treatment.....	53
Figure 4.20	Effect of 6BIO treatment on active and total Rac1 expression	54
Figure 4.21	Effect of 6BIO on Rac1.....	55
Figure 4.22	Images of Skbr3 spheroids treated with 6BIO	56
Figure 4.23	Reduction of the metabolism of spheroids by 6BIO	56
Figure 4.24	Reduction of migration and invasion of Skbr3 spheroids by 6BIO.....	57
Figure 6.1	Effects of 6BIO on metastatic signaling in tumor cells.....	66

INDEX OF TABLES

Table 1	Drugs based on natural products at different stages of development.....	3
Table 2	Top 32 kinase structures targeted by indirubin derivatives according to ligand docking.....	8
Table 3	Biochemicals, inhibitors, dyes and cell culture reagents	21
Table 4	Commonly used buffers.....	22
Table 5	Technical equipment	22
Table 6	Buffers for FCM analysis	24
Table 7	Buffers for preparation of total cell lysates.....	30
Table 8	Buffers and gels for Western blotting	31
Table 9	Tank buffer	32
Table 10	Primary antibodies.....	33
Table 11	Secondary antibodies.....	33
Table 12	Gel staining solution	34

ABBREVIATIONS

ANOVA	analysis of variance between groups
APS	ammonium persulfate
ATP	adenosine-5'-triphosphate
5BIO	5-bromoindirubin-3'-monoxime
6BIO	6-bromoindirubin-3'-monoxime
7BIO	7-bromoindirubin-3'-monoxime
BSA	bovine serum albumine
CDKs	cyclin dependent kinases
CSLM	confocal laser scanning microscopy
DMSO	dimethyl sulfoxide
DTT	dithio-1,4-threitol
ECL	enhanced chemoluminescence
ECM	extracellular matrix
EDTA	ethylenediaminetetraacetic acid
EGTA	ethylene glycol tetraacetic acid
FAK	focal adhesion kinase
FCS	foetal calf serum
FCM	flow cytometry
FL	fluorescence
GI	growth inhibition
GSK3 β	glycogen synthase kinase 3 β
HEPES	N-(2-hydroxyethyl)piperazine-N'-(2-ethanesulfonic acid)
HFS	hypotonic fluorochrome solution
IO	indirubin-3'-monoxime
kDa	kilo Dalton
MMP	matrix metalloproteinase
MTT	3-(4,5-dimethylthiazol-2-yl)-2,5-diphenyl tetrazolium bromide
NEAA	non-essential amino acids
PAA	polyacrylamide
PBS	phosphate-buffered saline
PDK1	3-phosphoinositide-dependent protein kinase 1
PH	pleckstrin homology
PI	propidium iodide
PI3K	phosphoinositide 3-kinase
PMSF	phenylmethylsulfonylfluorid
phos.	phosphorylated
PolyHEMA	polyhydroxyethylmethacrylate
PtdIns	phosphatidylinositol
Rac1	Ras-related C3 botulinum toxin substrate 1
RhoA	Ras homolog gene family, member A
SDS	sodium dodecyl sulphate
SDS-PAGE	sodium dodecyl sulphate polyacrylamide gel electrophoresis
SEM	standard error mean
SSC	sideward scatter
Stat3	signal transducer and activator of transcription 3
TBS-T	Tris buffered saline with tween
TEMED	N, N, N' N' tetramethylethylene diamine
T/E	Trypsin/EDTA
UV	ultraviolet
WB	Western blot

1 INTRODUCTION

1.1 Background: New aspects of anticancer drug discovery

According to the National Cancer Institute (NCI) cancer is defined as a term for diseases in which abnormal cells divide without control, showing the potential to invade nearby tissues or to spread to other parts of the body through the blood and lymphatic systems.

Evolving studies with several different targeted therapeutic agents are demonstrating that patients with genomic alterations of the target – including amplification, translocation and mutation – are more likely to respond to the therapy. Recent studies indicate that numerous components of the phosphatidylinositol-3-kinase (PI3K)/Akt pathway are altered by amplification, mutation and translocation more frequently than any other pathway in cancer patients, with resultant activation of the pathway. This warrants exploiting the PI3K/Akt pathway for cancer drug discovery.¹

The Akt signaling pathway has been implicated in several cytoskeleton-mediated processes including the regulation of actin reorganization during vascular endothelial growth factor (VEGF)-induced migration of endothelial cells² and blocking of ezeirin, a cytoskeleton-plasma membrane linker protein which negatively regulates Akt activity to promote apoptosis.³ Activated PI3K generates phosphoinositides which stimulate 3-phosphoinositide-dependent protein kinase 1 (PDK1) being attributed to phosphorylating T308 and possibly S473 on Akt.⁴ PDK1 is ubiquitously expressed in human tissues⁵ and its mediation in the PI3K/Akt pathways has been closely linked with several cancer types,⁶ especially breast cancer.⁷⁻⁸ Uncontrolled activation of the Akt pathway leads to a deregulation in cell growth and overall survival, allowing for competitive growth advantage, metastatic competence and, as often found in breast cancer, therapy resistance.⁹ This pathway is therefore an attractive target for the development of novel anticancer agents.^{1, 9-10}

In a recent inverse kinase screening assay looking for unexplored targets of newly derived substances, the PDK1 kinase was shown to be a target of the anticancer compound 6-bromo-indirubin-3'oxime (6BIO) – a synthetic derivative of the natural product indirubin – but not of 7-bromo-indirubin-3'oxime (7BIO) in endothelial cells.¹¹ As PDK1 kinase activity is directly responsible for the initial phosphorylation step in the full activation of Akt, it can be hypothesized that 6BIO could specifically target the deregulated pathways involving Akt in tumor cells.

Consequently, this preliminary study by Zahler et al.¹¹ prompted the investigation of two indirubin derivatives, namely 6BIO and 7BIO, in cancer cells in this thesis. As 6BIO, but not 7BIO, is able to bind to the PDK1 kinase with high affinity, the difference in target specificity will be used to demonstrate the essential role of Akt in metastatic tumor cells. Moreover, preliminary data will provide evidence of 6BIO's ability to repress the invasive capacity of tumor spheroids in a confrontation assay with human fibroblast spheroids.

1.2 The role of natural products in treatment of diseases

Natural products and compounds based on natural product structures are the single most prolific source of most drugs today.¹²⁻¹⁵ Over 100 natural product-derived compounds are currently undergoing clinical trials and at least 100 similar projects are in pre-clinical development. Most of these products are derived from plants and microbial sources as seen in Table 1.^{12, 16} Between 2005 and 2007, 13 natural product drugs were approved, five of which represent the first members of new classes of drugs.¹²⁻¹³

Table 1. Drugs based on natural products at different stages of development

Development stage	Plant	Bacterial	Fungal	Animal	Semi-synthetic	Total
Preclinical	46	12	7	7	27	99
Phase I	14	5	0	3	8	30
Phase II	41	4	0	10	11	66
Phase III	5	4	0	4	13	26
Pre-registration	2	0	0	0	2	4
Total	108	25	7	24	61	225

Source: Harvey 2008, Pharmaprojects database (March 2008).

Throughout history, natural products have had an essential role in the treatment of diseases. Egyptian medicine dates back to 2900 BC, but the best known record is the “Ebers Papyrus”, which dates from 1500 BC and documents over 700 drugs, mostly of plant origin. Records documenting the uses of approximately 1000 plant-derived substances in Mesopotamia date from around 2600 BC, and many are still used today for the treatment of ailments ranging from coughs and colds to parasitic infections and inflammation.¹⁷ Plants are of special note, with an extensive history in the treatment of cancer. It is reported by the World Health Organization (WHO) that over 3000 species of plants have been used in the treatment of cancer.¹⁸ A recent WHO survey of plant-derived pure compounds used as drugs in countries that contain WHO-Traditional Medicine Centers indicated that 80% of 122 compounds from 94 identifiable plant species were found to be used for the same or closely related ethnomedical purposes worldwide.^{14, 19-20} These findings show that natural products have played an essential role in helping to define natural product sources used in contemporary medicines.

There are many historical examples in which the natural product has not just been the medicinal product, but has also helped to reveal a novel aspect of physiology. For example, Digitalis from foxglove enabled the elucidation of the role of sodium-potassium-ATPase.^{12, 21} Furthermore, Taxol which surprisingly stabilizes microtubules during cell division rather than destabilizing them as Vinblastine does, allowed the establishment of structure–activity relationships for hundreds of semi-synthetic analogues.²² By elucidating and understanding mechanism such as these, drug discovery can be specifically targeted towards deregulated systems in various diseases, especially cancers.

1.3 Indirubins as anticancer compounds

Indirubins are highly promising novel anticancer compounds derived from natural products which inhibit cyclin dependent kinases (CDKs) preferentially. CDKs are a family of small serine/threonine kinases that associate with cyclins and are generally known as the master regulators of the main transitions of the eukaryotic cell cycle.²³ CDKs are often deregulated in cancer making them interesting targets for chemotherapeutics. Several recent indirubin derivatives have also been shown to interact with key members of pathways which are involved in the development of cancer including 3-phosphoinositide-dependent protein kinase 1 (PDK1), glycogen synthase kinase 3 β (GSK3 β), protein kinase C (PKC) isoforms, protein kinase A (PKA), and c-Src tyrosine kinase. These compounds are very promising candidates that need to be fully investigated, so that they can reach the clinic.

1.3.1 History of indirubins

Indigoids are a chemical family of bis-indoles based on indigo, indirubin and their collective derivatives. The family of indigoids has had a noteworthy pharmaceutical, historical and a substantial cultural impact.²⁴⁻²⁵ Indirubin is derived from a spontaneous non-enzymatic dimerisation of isatin and indoxyl, both of these precursors are found in various natural sources including marine mollusks, bacteria, indigo-producing plants, and is sometimes present in mammalian urine which is also known as “purple bag syndrome.”²⁴⁻²⁹

Danggui Longhui Wan is a traditional Chinese medicinal preparation which contains eleven herbal constituents used to treat various chronic diseases including chronic myeloid leukemia. Recent interest in the Chinese pharmacopeia has led to the discovery of the active herbal component of this mixture named Qing Dai or better known as indigo naturalis. It is the red colored byproduct 3, 2' isomer indirubin and has found to be the main antileukemic component of this herb.²⁸ Indirubin itself was described more than 30 years ago as a treatment for chronic myeloid leukemia.³⁰

Several research groups have intensively studied indirubins and some of their derivatives to try and elucidate their complex modes of action. Different members of the indirubin family act as potent inhibitors of CDKs,²⁹ glycogen synthase kinase 3 (GSK3),³¹⁻³² the aryl hydrocarbon receptor (AHR),²⁶ the Src tyrosine kinase and the Stat3 transcription factor³³ among other yet-undefined targets.

Also, indirubins have been pursued in both animal and human studies. Membrane morphology of the surface of white blood cells of guinea pigs treated with indirubins has been reported to be altered.³⁴ The absence of bone marrow toxicity and hematotoxicity was found in long term animal studies³⁵⁻³⁶ and reversible diarrhea and slight hepatotoxicity were seen over a 6 month study in dogs with indirubin doses up to 25 times higher than those used for treatment in humans.^{28, 36}

Indirubin itself is no longer in clinical use due to its poor water solubility, but a wide variety of derivatives have been chemically synthesized to optimize selectivity, solubility and efficacy against tumor growth.³¹

1.3.2 6BIO and 7BIO: Specific derivatives of indirubins

The lack of cellular uptake of indirubin is unfavorable and has led to a wide variety of modified derivatives in search of improved cellular membrane permeability. Introduction of an oxime group in position 3' allowed the generation of β -glycosides linked through an ethylene ether bridge is a very promising approach into novel drugs with improved bioavailability as these substances tend to preferentially inhibit CDKs and other kinases.²⁸

Crystal structures of CDK2, a kinase that is involved in cell cycle control, in complex with indirubin-3'-oxime (IO) have recently been published.^{29, 37} The interaction of the inhibitor with the ATP-binding site was characterized and the bent shape of indirubin 'facial side' complements the shape of the ATP-binding pocket.³⁷ Additionally, three derivatives, namely 5-bromo-indirubin-3'-oxime (5BIO), 6-bromo-indirubin-3'-oxime (6BIO), and 7-bromo-indirubin-3'-oxime (7BIO) – although incredibly similar on a structural level – have been reported to have significantly varied biological activities. Both 5BIO and 6BIO are reported to inhibit CDKs, GSK-3 β and other kinases,³¹ whereas 7BIO was shown to induce cellular death in a kinase-independent manner.³⁸⁻³⁹

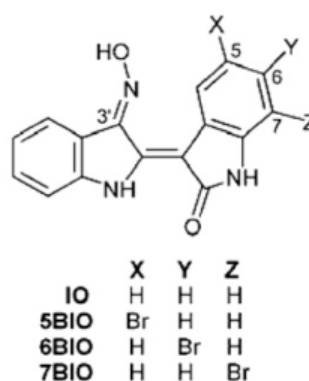


Figure 1.1: 2D Structure of indirubin derivatives

Image adapted from Zahler et al.¹¹

6BIO (Figure 1.1) was reported by Meijer et al. in 2003³¹ as a synthetic derivative from the natural product 6-bromoindirubin which was discovered as an active component extracted from the "Tyrian purple" dye produced from gastropod mollusks. It was described therein as a potent and selective inhibitor for GSK-3 β . Co-crystal structures of 6BIO and GSK-3 β as well as 6BIO and CDK2 were published showing 6BIO interacting within the ATP-binding pockets of these kinases.³¹

Since this landmark paper, there have been just over 40 publications focusing on 6BIO activity in neurons,^{32, 40} against bone loss,⁴¹ in liver tissues,⁴² in cardiomyocytes,⁴³ as well as in Wnt and Stat3 signaling pathways.^{33, 42, 44-45}

Quite recently the substance was used to expand stem cells and maintain their self-renewal.⁴⁵⁻⁴⁷ As it is such a new compound, only a few of the kinase targets have been elucidated and further study is essential to fully understand its antitumor capabilities.

Although nearly structurally identical to 6BIO, the substance 7BIO (Figure 1.1) has been reported to have a completely different mode of action as an antitumor compound relative to other reported indirubin derivatives.³⁸ It was demonstrated to induce cellular death, possibly through necrosis or autophagy, rather than the typically studied indirubin targets of CDKs or GSK-3 β .³⁹ Very limited information on this substance has been published so far, and its modes of action are not well defined.

1.3.3 Kinase screening with indirubin derivatives

The basis for my thesis came from a recent report out of our lab in which several indirubin derivatives were investigated in a virtual kinase screening assay which was supported with an *in vitro* kinase assay.¹¹

The first assay was a digital inverse kinase screening assay against a database of approximately 6000 protein binding sites. Single compounds were docked into protein structures stored within the database, and the top 32 protein binding sites for each compound are shown in Table 2.

The outcome of this assay indicates that both 5BIO and 6BIO show strong binding to their already defined targets (CDK2, CDK5 and GSK-3 β), with several other major targets in the top 1% as potential targets (CSK2A, WEE1, CDC2H, RIFK and PDK1). Specifically, in the inverse screening assay, 6BIO seemed to target PDK1 much more effectively than the other indirubin derivatives tested. These findings were briefly experimentally validated and 6BIO was shown to be the only potentially effective derivative as an inhibitor of PDK1.

Table 2. Top 32 kinase structures targeted by indirubin derivatives according to ligand docking(Table Source: Zahler et al. 2007¹¹)

5 BIO			6 BIO			7 BIO		
PDB ID	Kinase	Score	PDB ID	Kinase	Score	PDB ID	Kinase	Score
1pxo_CK7	CDK2	-8.878	1q41_IXM	GSK3B	-8.731	1waw_RIG	CHIT1	-8.082
1jvp_LIG	CDK2	-8.472	2bhe_BRY	CDK2	-8.617	1nb9_RBF	RIFK	-8.052
1w0x_OLO	CDK2	-8.456	1jvp_LIG	CDK2	-8.497	2bqz_SAH	SETD8	-7.821
1e9h_INR	CDK2	-8.390	1unh_IXM	CDK5	-8.444	2bqz_SAH	SETD8	-7.821
1pkd_UCN	CDK2	-8.352	1x8b_824	WEE1	-8.337	1jvp_LIG	CDK2	-7.765
1q41_IXM	GSK3B	-8.318	1pye_PM1	CDK2	-8.263	1x8b_824	WEE1	-7.719
1fin_ATP	CDK2	-8.217	1r78_FMD	CDK2	-8.097	1m6w_12H	ADHX	-7.689
1x8b_824	WEE1	-8.160	1e9h_INR	CDK2	-7.983	1zkk_SAH	SETD8	-7.684
1pxp_CK8	CDK2	-8.108	1waw_RIG	CHIT1	-7.983	1q91_DPB	NT5M	-7.671
1pye_PM1	CDK2	-8.076	1waw_RIG	CHIT1	-7.983	1tbm_IBM	PDE9A	-7.671
1vyw_292	CDK2	-8.054	1oky_STU	PDK1	-7.975	1s1r_NAP	AK1C3	-7.664
1waw_RIG	CHIT1	-8.050	1fin_ATP	CDK2	-7.967	1s1p_NAP	AK1C3	-7.654
1xbc_STU	KSYK	-8.003	1nb9_RBF	RIFK	-7.897	1q41_IXM	GSK3B	-7.531
1xp0_VDN	PDE5A	-7.962	1aq1_STU	CDK2	-7.885	1v40_O16	PTGD2	-7.531
1nb9_RBF	RIFK	-7.922	1dig_L37	C1TC	-7.881	1w0x_OLO	CDK2	-7.515
1sm2_STU	ITK	-7.839	1xbc_STU	KSYK	-7.874	1r0p_KSA	MET	-7.482
1dig_L37	C1TC	-7.770	1dia_L24	C1TC	-7.827	1pjk_ANP	CSK21	-7.474
1aq1_STU	CDK2	-7.742	1udt_VIA	PDE5A	-7.802	1n6a_SAM	SETD7	-7.431
1oky_STU	PDK1	-7.729	1tbf_VIA	PDE5A	-7.784	1x97_FIR	ALDR	-7.369
1u59_STU	ZAP70	-7.724	1y6a_AAZ	VGFR2	-7.768	1z57_DBQ	CLK1	-7.319
1oit_HDT	CDK2	-7.674	1q91_DPB	NT5M	-7.747	1mlw_HBI	TPH1	-7.309
1pjk_ANP	CSK21	-7.673	1oiq_HDU	CDK2	-7.726	1pwm_FID	ALDR	-7.297
1tbf_VIA	PDE5A	-7.628	1di8_DTQ	CDK2	-7.717	1uyf_PU1	HS90A	-7.295
1h1s_4SP	CDK2	-7.621	1urw_I1P	CDK2	-7.707	1p2a_5BN	CDK2	-7.257
1y6a_AAZ	VGFR2	-7.597	1xg5_NAP	DHR11	-7.698	1dig_L37	C1TC	-7.220
1xu7_NDP	DHI1	-7.544	1uu7_BI2	PDK1	-7.698	1el3_I84	ALDR	-7.215
1dia_L24	C1TC	-7.539	1jqe_QUN	HNMT	-7.690	1cea_ACA	PLMN	-7.171
2bqz_SAH	SETD8	-7.523	1uho_VDN	PDE5A	-7.657	1xqh_SAH	SETD7	-7.168
1xu9_NDP	DHI1	-7.518	2bqz_SAH	SETD8	-7.646	1ish_ENP	BST1	-7.160
1pwm_FID	ALDR	-7.509	2biy_ATP	PDK1	-7.610	1pye_PM1	CDK2	-7.137

Ligands were docked to the structures in the Protein Data Base, with the PDK1 kinase highlighted in gray. Abbreviations under PDB ID: STU (staurosporine), IXM (indirubin-3'-monoxime), and ANP (phosphoaminophosphonic acid-adenylateester). All kinase structures are listed with most favorable docking scores in descending order.

Additionally, Figure 1.2 depicts virtual examples of the docking assay.¹¹ The images indicate that indirubin 3'-oxime (IO) shows a strong binding preference for CDK2 in Figure 1.2(B) and the ability to bind to CDK5 in Figure 1.2(A). 6BIO is shown docked to PDK1 in the presence of staurosporine in Figure 1.2(C) or with PDK1 alone using VDW-Sphere imaging in Figure 1.2(D). Moreover, 7BIO is docked to PDK1 with the LY333531 inhibitor, but the binding is not optimal (Figure 1.2(E)).

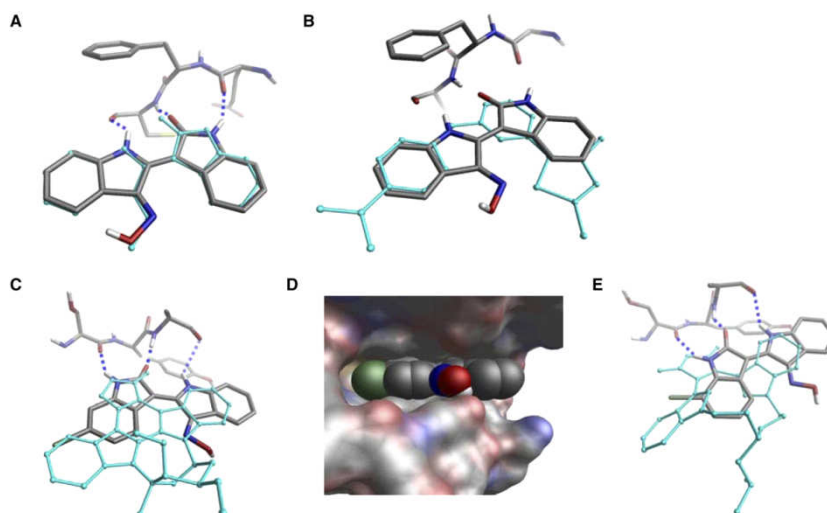


Figure 1.2: Docking assay results

A) Indirubin 3'-oxime (thick, atom colored sticks) redocked into a CDK5 structure in complex with indirubin 3'-oxime. The resulting score leads to rank 11 for this structure among the kinases and 36 in the complete set of complexes. The model is in perfect agreement with the typical interaction motif of two or three hydrogen bonds (shown as dashed blue lines) to the protein backbone (shown in the background of this picture). The conformation of indirubin 3'-oxime as found in the PDB structure is shown as thin cyan sticks and shows nearly perfect agreement with the model. B) Indirubin 3'-oxime (thick, atomcolored sticks) docked into a CDK2 structure. This complex has rank 1 among the kinases and rank 5 in the complete set. The model is in perfect agreement with the typical interaction motif of two or three hydrogen bonds (shown as dashed blue lines) to the protein backbone (shown in the background of this picture). The ligand originally contained in the X-ray structure is shown as thin cyan sticks for comparison. C) 6-bromo-indirubin 3'-oxime model into PDK1 with bound inhibitor staurosporine. The figure shows the good agreement with the backbone hydrogen bonding motif. D) The solvent accessible surface of the binding pocket of PDK1 together with the VDW-Sphere depiction of 6-bromo-indirubin 3'-oxime indicate that the binding pocket can easily accommodate the halogen. E) 7-bromo-indirubin 3'-oxime docked into PDK1 with bound inhibitor LY333531. The binding motif is in principle present; however, the geometry of the hydrogen bonds to the backbone is not optimal. Image adapted from Zahler et al.¹¹

Finally, based on the results from the virtual kinase screening assay, an *in vitro* PDK1 kinase assay was performed. Figure 1.3 shows the results of a collaborative effort between our lab, the Bioinformatics group at the Department of Computer Science at LMU and ProQinase GmbH.¹¹ The graphs indicate that there is a dose-

dependent relationship with PDK1 kinase and that 6BIO (IC_{50} value of 1.5 μM) is the most optimal of the four indirubin derivatives tested.

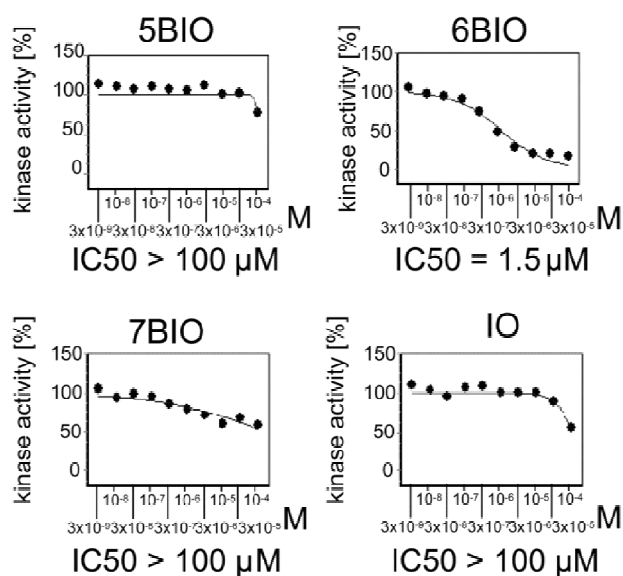


Figure 1.3: *In vitro* kinase assay results

Dose-response relationships for the three compounds in the *in vitro* kinase assay for PDK1. 5BIO and 7BIO show inhibition only at the highest concentration tested (100 μM), whereas 6BIO shows a classical sigmoidal curve with an IC_{50} of 1.5 μM .

1.4 Metastatic cancer: Treatments and targeted mechanisms

In women, breast cancer is the most common form of cancer, with a current lifetime risk of one in every eight women developing breast cancer.⁴⁸ It is second only to lung cancer as cause of cancer death among women of all races, with metastatic breast cancer continuing to be reported as incurable.⁴⁹ Both recent clinical and molecular studies have indicated that circulating tumor cells can be detected early in the development of the breast tumor.⁵⁰ Additionally, according to the NCI, pancreatic cancer which is one of the most horrific forms of metastatic cancer, had just under 43,000 newly reported cases and over 35,000 deaths attributed to this cancer alone in 2009. Mortality rates in metastatic cancer are primarily due to metastases and invasion of the surrounding tissues by migrating tumor cells rather than to the primary tumors themselves.⁵¹ Therapeutic intervention should be targeted towards the highly proliferic and metastatic pathways in tumor cells to efficiently reduce mortality rates.

1.4.1 Standard treatments for metastatic cancer

Initially, the surgical removal of tumors or use of radiotherapy can provide or even cure some cancers. These therapies are limited in that they are only capable of targeting local or regional tumors. Metastatic cancer, however, requires the use of cytotoxic chemotherapies, targeted therapies or therapies tailored to hormone imbalance to treat the tumors which have spread throughout the body. While sometimes effective, these treatments can be associated with severe toxic side effects, or the cancer cells themselves can become resistant to the chemotherapeutic agents.

Current methodologies of treatment of metastatic cancer can be broken down into three major chemotherapeutic categories in combination with standard surgical and radiotherapeutic techniques.⁵²

- Cytotoxic chemotherapies - include the well-known substances of Paclitaxel, Doxorubicin and 5-Fluorouracil. These substances are able to disrupt cellular functions in dividing cancer cells.⁵³
- Targeted therapies – include Bevacizumab or Trastuzumab, both of which are monoclonal antibodies capable of targeting specific over-expressed oncogenes in metastatic tumor cells.⁵⁴ These forms of therapies are now becoming more popular due to their success rates and specific targeting of tumor cells.
- Hormonal therapies – include substances such as Raloxifene or Fulvestrant. This form of therapy works only in the specific case of cancers that grow in the presence of estrogen (ER) or progesterone (PR). They are most often used for ER+ or PR+ tumors.⁵⁵

Each of these treatment categories has varied levels of success rate dependent on tumor type and any previous treatments. In many cases the success rates are rather low and often associated with very serious secondary effects making the search for anti-metastatic chemotherapeutics a top priority in the fight against cancer.

1.4.2 Regulation and signaling of tumor cell migration

To achieve metastasis, cancer cells must evade or co-opt multiple rules and barriers. Therefore metastatic signaling is an extremely complex process of events which cancer cells undergo. Several discrete steps are discernible in the biological cascade of metastasis: loss of cellular adhesion, increased tumor cell motility and invasiveness, entry and survival in circulation, exit into new tissue, and eventual colonization of a distant site.⁵⁶ Figure 1.4 depicts the currently accepted model of metastatic tumors.

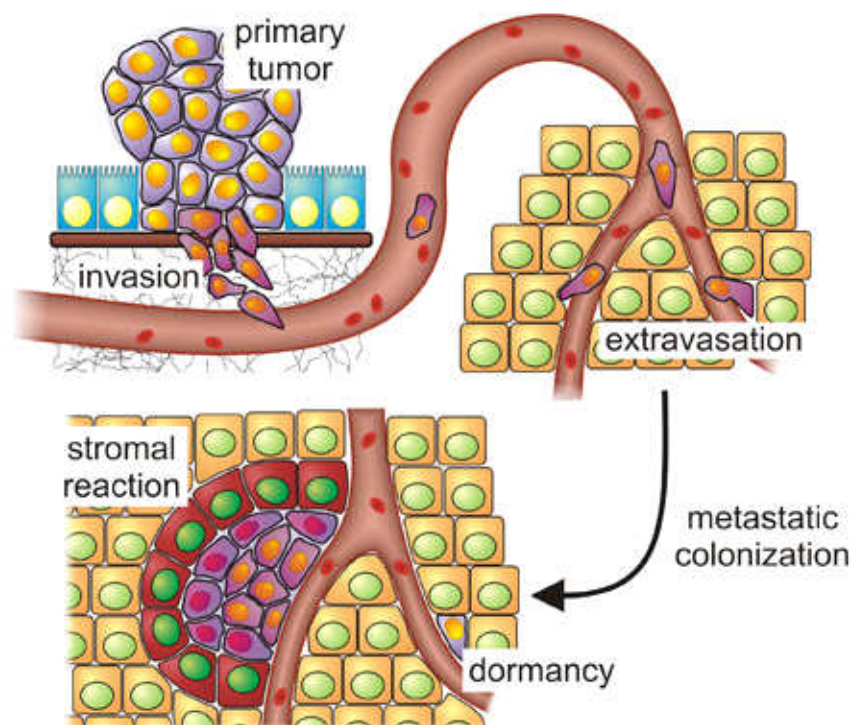


Figure 1.4: Basic overview of metastatic signaling

Cells from the primary tumor gain migratory properties and invade into the surrounding stroma in the initial phases of the metastatic cascade. Following circulation, the cells must actively extravasate into the target organ. Once in the new location, the cells must activate the surrounding stroma and either persist in a dormant state or die. Image adapted from Dr. Y Shiozawa⁵⁷

During cellular migration the initial step is the polarization of the cell using actin-dependent protrusions found at the leading edge of the cell, where the lamellipodia and filopodia are formed. Next, integrin clustering at new adhesion points attach to the substratum are formed under the leading edge during the cellular extension phase. Ras-related C3 botulinum toxin substrate 1 (Rac1), a member of the Rho family of GTP-binding proteins, is activated and contributes to the polarity and shape of the migrating cell. This phase is followed by the translocation of the nucleus and the cell body towards the front of the cell by the actomyosin-based contraction forces linked to the integrin clusters found at the focal adhesions. Finally in the retraction phase, the retraction fibers draw the rear of the cell forward in conjunction with the disassembly of the focal adhesions now found at the rear of the cell as seen in Figure 1.5.

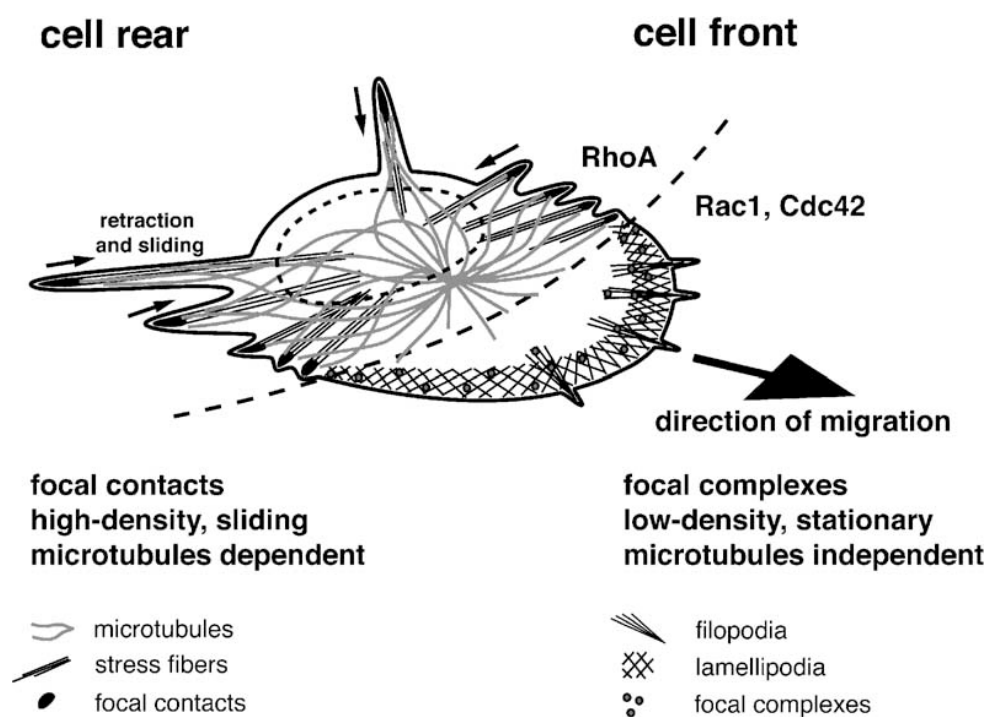


Figure 1.5: Cell migration

Image of cellular migration depicting the cell polarization at which focal contacts form at the leading edge of the cell. Protrusion and new focal adhesion formation at the leading edge of the cell and rear retraction and adhesion disassembly at the rear of the cell. Image adapted from Wehrle-Haller 2003.⁵⁸

1.4.2.1 The actin cytoskeleton

The actin cytoskeleton is essential in regulating the basic cellular infrastructure as well as its key role in motility.⁵⁹ The three main types of cytoskeletal proteins include microtubules, intermediate filaments and actin filaments.

The first step in migration is polarization of the cell. During this step the filopodia and lamellipodia, which are actin-dependent protrusions, begin to form structures at the leading edge of the cell. Filopodia are the thin projections of plasma membrane supported by actin bundles. Lamellipodia are the broad, ruffle-like membrane protrusions observed at the leading edge of cells during movement. Integrins are responsible for cellular attachment to and movement along the extracellular matrix (ECM), which causes reorganization of the actin cytoskeleton.⁶⁰⁻⁶¹ On ligation to the ECM, integrins cluster in the plane of the membrane and recruit various signaling and adaptor proteins to form structures known as focal adhesions (FAs) which also serve as attachment sites for recruitment proteins and large bundles of actin filaments called stress fibers.⁶²

Actin is a 43-kilodalton (kDa) protein which forms actin filaments (F actin) through a complex process of polymerization and depolymerization. These filaments elongate through the reversible addition of monomers to either end, with the plus end elongating at a faster rate than the minus end. This effect occurs because ATP-actin dissociates less readily than adenosine diphosphate (ADP)-actin. Due to this variance in rate, there is a significant variance in the critical concentration of monomers at either end, resulting in what is known as treadmilling. Treadmilling is an essential part of the dynamic assembly and disassembly of F actin filaments which is required for both structure and movement.^{59, 63}

Figure 1.6 depicts an actin model of cellular migration. Lamellipodia and filopodia are shown on the leading edge of the cell. The contraction of the F actin stress fiber network drives the cell forward in response to integrin-mediated signaling at the FAs. Key regulators control the actin-binding proteins, regulating the necessary assembly, disassembly and cross-linking of actin filaments.^{58-59, 63} Members of the Rho subfamily of small GTP-binding proteins (GTPases) in conjunction with focal adhesions and integrins play key roles in cancer cell motility by regulating the

organization of the actin cytoskeleton, thus controlling a variety of cell processes, including cell motility, cell adhesion and cytokinesis.^{58, 64-66}

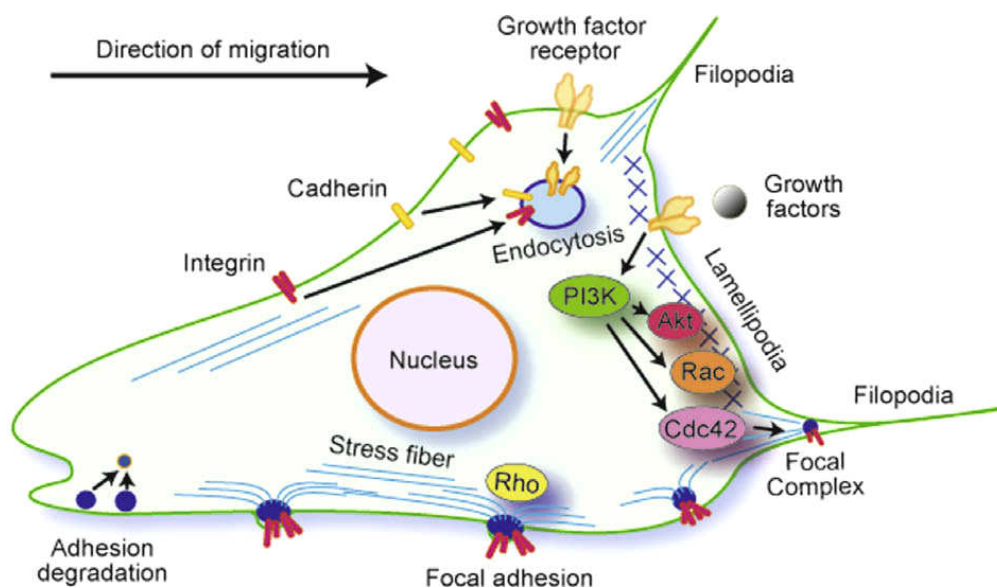


Figure 1.6: Cell motility model

Lamellipodia form at the leading edge upon integrin signaling. Focal adhesions are formed and F actin stress fibers contract to drag the cell forward in conjunction with the disassembly of the adhesions at the rear of the cell. The cell is then dragged in the direction of migration. Integrins are endocytosed and recycled to the leading edge of the cell during movement. PI3K is activated in response to growth factors leading to the recruitment of active Akt to the leading edge where the lamellipodia are further induced by Rac1. Image adapted from Jiang 2009.⁶⁴

Furthermore, integrins are responsible for cellular attachment to and movement along the extracellular matrix (ECM), which causes the reorganization of the actin cytoskeleton.⁶⁰⁻⁶¹ On ligation to the ECM, integrins cluster in the plane of the membrane and recruit various signaling and adaptor proteins to form structures known as focal adhesions which also serve as attachment sites for recruitment proteins and large bundles of actin filaments called stress fibers.⁶²

1.4.2.2 Akt as a cellular key regulator

Akt, also known as protein kinase B, is a 57 kDa serine/threonine kinase which has recently been shown to be an essential regulator of the actin cytoskeleton during cellular migration.⁶⁷ Additionally, Akt is known to play a crucial role in cell survival, growth, proliferation, angiogenesis and cellular metabolism as well as in cell migration and invasion.^{6, 67-69}

Growth factors are thought to be necessary for the full activation of Akt. These growth factors bind to receptors and activate the receptor-associated PI3K which phosphorylates PtdIns-3,4-P₂ to PtdIns-3,4,5-P₃. The hydrophilic portion of the PtdIns-3,4,5-P₃ binds to the PH domain of Akt, whereas the hydrophobic part of the PtdIns-3,4,5-P₃ interacts with lipid bilayer of the membrane thus translocating Akt to the plasma membrane. This translocation brings it into the proximity of both the PI3K-dependent kinase 1 (PDK1) and PDK2 which, in the case of PDK1, is thought to be constitutively active and mutually co-localizes with the PtdIns-3,4,5-P₃ to the plasma membrane.⁷⁰ Akt thereby undergoes phosphorylation at two sites, first at the activation loop (T308) and then at the carboxy-terminal tail (S473). Phosphorylation at T308 is attributed solely to the action of PDK1. The kinase that phosphorylates Akt at S473 (PDK2) has been discussed for many years and has been attributed the mTOR complex, PDK1, Akt itself or other members of the AGC family.⁷¹⁻⁷⁴ Akt is considered fully activated only when both the T308 and the S473 have been phosphorylated (Figure 1.7).

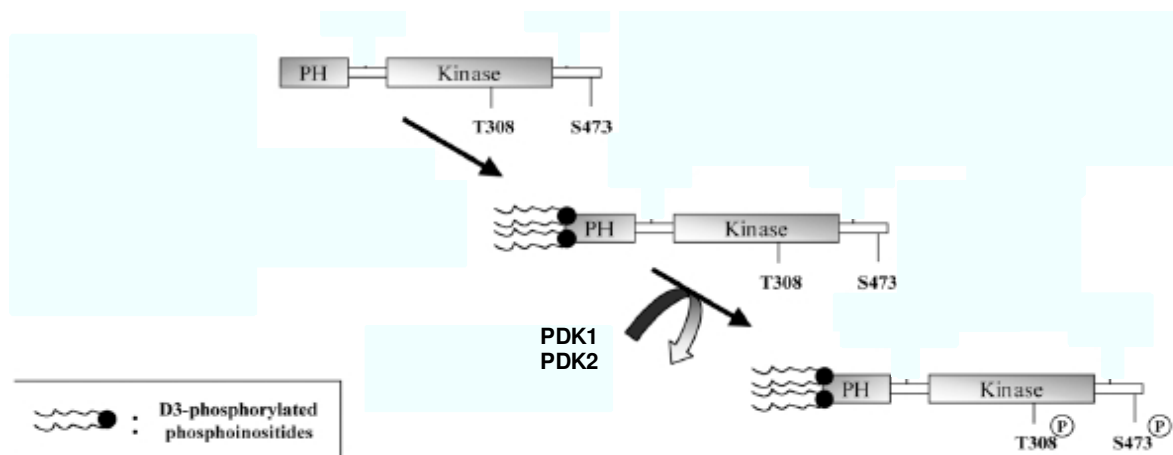


Figure 1.7: Model of Akt and Akt activation

PtdIns interact with the PH domain of Akt to promote the translocation of Akt from the cytosol to the plasma membrane. PDK1 interacts with the C-tail and phosphorylates T308. The S-residue at position 473 is phosphorylated by PDK2. This final form of Akt is fully active and can phosphorylate target proteins.

Image adapted from Grille 2003.⁷⁵

Upon complete activation, Akt is released back into the cytoplasm where it activates a number of substrates. It has been linked to the inside-out activation of integrins in endothelial cells and fibroblasts, which in turn, mediates matrix assembly as well as regulating fibronectin assembly through the activation of $\alpha 5\beta 1$ integrin.⁶⁷ Akt has been shown to regulate the recycling of $\alpha 5\beta 1$ integrin from the lagging edge to the lamellipodia in fibroblasts which leads to enhanced migration.^{67, 76} In a similar report, Akt knockout cells showed lower levels of proliferation as well as an impairment in migration and in extracellular matrix response.⁷⁷

1.4.2.3 $\beta 1$ Integrin as a main mediator of cell migration

Integrins are transmembrane receptors that mediate attachment between a cell and the tissues or cells surrounding it. They bind the surface of a cell to ECM components including fibronectin, laminin and collagen. They have a central role in signaling pathways that define the shape of the cell, the migration of the cell, and have been reported to help regulate the cell cycle.⁷⁸⁻⁸⁰

The family of integrins contains 8 beta and 18 alpha subunits. As they are obligate heterodimers, the subunits assemble in pairs making up 24 distinct integrin combinations. Every integrin is comprised of the two subunits and will only recognize relatively short peptide motifs on their respective ligands. The 24 integrin combinations appear to have clear, non-redundant functions, shown through the generation of an extensive series of knockout mice.⁷⁸

Integrins perform outside-in signaling, but they also operate an inside-out signaling. This means that they are capable of transducing information from the ECM to the cell as well as reveal the status of the cell to the outside, allowing rapid and flexible responses to changes in the environment.⁷⁸ Figure 1.8 shows a basic model of integrin structure and activation.

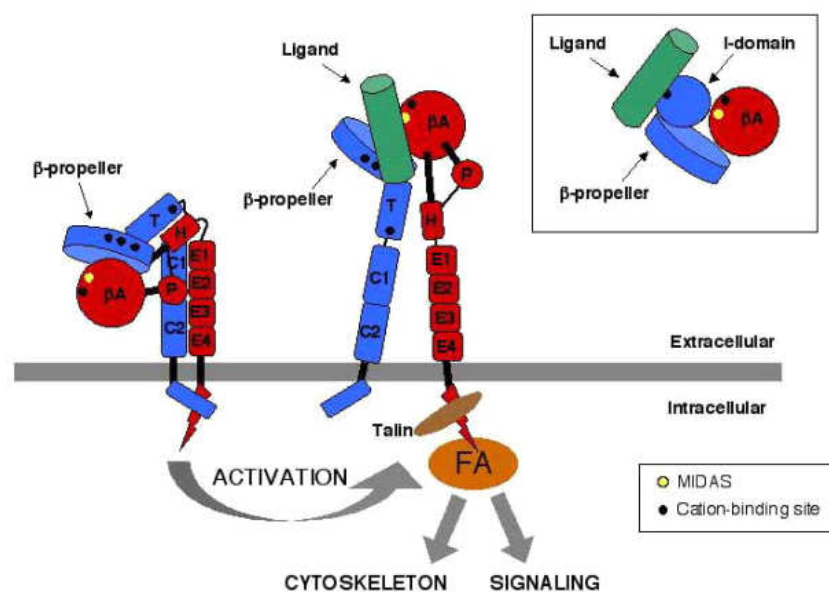


Figure 1.8: Structure and activation of integrins

Integrins consist of a 'head' region and two 'legs'. The heads contains a 'beta propeller' domain (alpha subunit) and a 'propeller-like' domain (beta subunit). A large interface between these two domains allows for stable association of heterodimer. In some alpha subunits, an I domain is inserted into the beta propeller domain and participates in promoting ligand binding (insert). The 'legs' consist of tightly packed domains that form a rigid stalk with a flexible hinge region. Five cation-binding sites are located within the head while a sixth one is present on the alpha subunit near the hinge region. The inactive, non-ligand occupied integrin is bent at the 'knee' region, and the 'head' domain faces down toward the membrane with the ligand-binding pocket in a low affinity conformation. The association of the alpha and beta cytoplasmic domains retains the integrin in the resting state. Talin binding to the beta cytoplasmic domain disrupts this alpha -beta cytoplasmic interaction, and triggers the inside-out conformational change leading to receptor activation. Activation is associated with slight shifting movement of the alpha and beta 'stalk' regions relative to each other, unbending (stretching) of the 'knee' region, and transition of the ligand-binding pocket into a high-affinity conformation.

Image adapted from the Division of Experimental Oncology (Centre Pluridisciplinaire d'Oncologie Lausanne Cancer Center)

In breast cancer and several other tumor types, an over-expression of specific integrins has been linked to increased disease progression and decreased patient survival.⁶² $\alpha\beta1$ Integrin has been observed numerous times in a variety of cell lines, indicating that it is essential for binding to fibronectin. It potentially participates through binding with the FAK/PI3K/Akt cascade to regulate tumor cell migration as depicted in Figure 1.9.^{66, 78, 81-82} Moreover, Akt was shown to regulate the endocytosis and recycling of integrins through the phosphorylation of ACAP1. Upon phosphorylation by Akt, the ACAP1 binds directly to the $\beta1$ integrin on endosomal membranes to promote integrin recycling and therefore cell migration.^{64, 83}

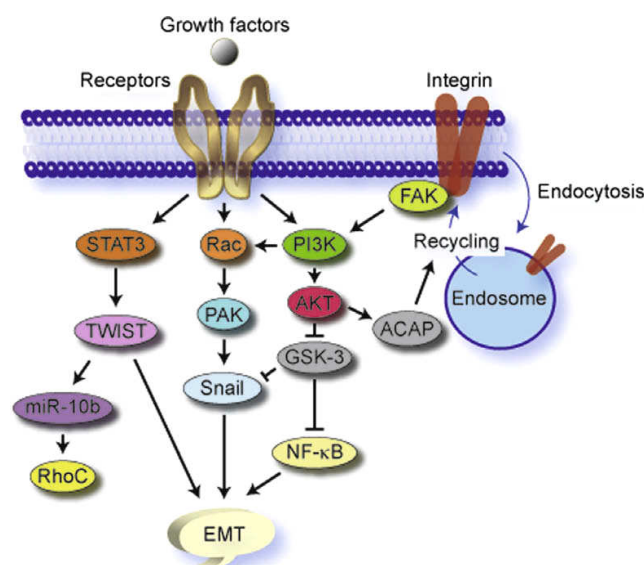


Figure 1.9: Integrin regulation and recycling

Growth factors and integrin-ligand interactions regulate cell movement through various intracellular routes. The activation of growth factor receptors triggers intracellular signaling cascades, leading to the activation or inactivation of a variety of downstream molecules responsible for EMT. FAK activation by integrin-ligand interactions promotes PI3K/Akt signalling. The PI3K/Akt signalling pathway also promotes the recycling of integrins during cell migration via phosphorylation of ACAP1. Image adapted from P. Jian 2009.⁶⁴

The $\beta 1$ integrin cytoplasmic domain contains five potential phosphorylation sites, of which the S785 site was shown to be essential for focal adhesion formation. Mulrooney et al.⁸⁴ proposed a model for migration in which phosphorylation of $\beta 1$ integrin modulates the integrin-cytoskeleton interactions. In the dephosphorylated state, the $\beta 1$ integrin is capable of interacting with the actin-based cytoskeleton and the focal adhesion proteins to create a focal adhesion site. They further proposed that phosphorylation of S785 on $\beta 1$ integrin results in the breaking of this integrin-cytoskeleton link. Migration is promoted in part by the dynamic regulation of the phosphorylation state of S785 which regulated the integrin actin connection and therefore alterations in this delicate cycle will disrupt normal cellular migration.⁸⁴

To sum up, deregulated metastatic pathways in cancer lead to a higher incidence of cancer mortality due to secondary tumors. New substances are desperately needed to specifically target the spread of tumors as well as to trigger the built in apoptotic pathways. So far, both 6BIO and 7BIO have turned out to be promising antitumor agents, with 6BIO showing strong effects against tumor metastasis.

2 AIMS OF THE STUDY

Metastatic cancer is a horrific disease with little chance of a cure with available modern treatments. The small amount of research available for 6BIO and 7BIO indicate that they are potential candidates for clinical therapy, but further research is necessary to fully comprehend their anticancer abilities.

To further elucidate the underlying mechanisms involved, the major goals of this study were as follows:

a) Antitumor activities of 6BIO and 7BIO

For this aim a wide variety of *in vitro* assays were performed using FCM analysis to assess apoptosis and anoikis induction, as well as assays to monitor proliferation and viability upon exposure to the indirubin derivatives.

b) Effects of 6BIO and 7BIO on metastatic pathways

For this aim a variety of migratory assays in response to different chemoattractants were performed including wound healing, Transwell™ migration and chemotaxis assays. Additionally, adhesion to fibronectin and invasive capabilities through Matrigel™ were assessed.

c) Effects of 6BIO on migratory signaling targets

This aim was intended to look at which point the migratory signaling pathways were disrupted upon treatment with 6BIO.

d) Effects of 6BIO in different cell models

As 6BIO has been shown to have varying effects based on the cell line, two tumor cell lines and a 3D spheroid model with both tumor spheroids and human fibroblast spheroids were utilized to evaluate the anti-migratory ability of 6BIO.

3 MATERIALS AND METHODS

3.1 Materials

3.1.1 Study compounds: 6BIO and 7BIO

6BIO and 7BIO used in the initial experiments were kindly provided by Dr. Meijer (Roscoff Biological Station in France, CNRS), and further investigations were performed with 6BIO and 7BIO purchased from Enzo Life Sciences (Farmingdale, NY). Before stimulation, all substances were dissolved and further diluted in DMSO with final DMSO concentrations in all assays not exceeding 1%. All 10 mM stock solutions and substances were stored at -20°C until use.

3.1.2 Biochemicals, inhibitors, dyes and cell culture reagents

Table 3. Biochemicals, inhibitors, dyes and cell culture reagents

Reagent	Supplier
Accustain® formaldehyde	Sigma-Aldrich, Taufkirchen, Germany
Bradford Reagent™	Bio-Rad, Munich, Germany
Collagen G	Biochrome AG, Berlin, Germany
Complete®	Roche Diagnostics, Penzberg, Germany
DMSO	Roth GmbH, Karlsruhe, Germany
DMEM	PAN Biotech, Aidenbach, Germany
FCS gold	PAN Biotech, Aidenbach, Germany
Glutimate	PAN Biotech, Aidenbach, Germany
McCoy's Medium	PAN Biotech, Aidenbach, Germany
Matrigel™	BD Discovery, Bedford, MA, USA
MTT	Sigma-Aldrich, Taufkirchen, Germany
NEAA	Invitrogen, Karlsruhe, Germany
Page Ruler™ Protein Ladder	Fermentas, St. Leon-Rot, Germany
Penicillin	PAN Biotech, Aidenbach, Germany
Polyacrylamide	Roth GmbH, Karlsruhe, Germany
Propidium iodide	Sigma-Aldrich, Taufkirchen, Germany
PermaFluor mounting medium	Beckman Coulter, Krefeld, Germany
Pyruvate	Merck, Darmstadt, Germany
Rhodamin-phalloidin	Invitrogen, Karlsruhe, Germany
RPMI 1640	PAN Biotech, Aidenbach, Germany
Streptomycin	PAN Biotech, Aidenbach, Germany
Tris-HCl	Sigma-Aldrich, Taufkirchen, Germany
Triton X-100	Merck, Darmstadt, Germany

Table 4. Commonly used buffers

Trypsin/EDTA (T/E)		PBS (+)	
Trypsin	0.5 g	NaCl	7.20 g
EDTA	0.2 g	Na ₂ HPO ₄	1.48 g
PBS	1.0 L	KH ₂ PO ₄	0.43 g
H ₂ O	1.0 L, pH 7.4	MgCl ₂ x 6 H ₂ O	0.10 g
		CaCl ₂ x 2 H ₂ O	0.10 g
		H ₂ O	1.0 L, pH 7.4

3.1.3 Technical equipment

Table 5. Technical equipment

Name	Device	Producer
Axioskop	Upright microscope	Zeiss Jena, Germany
Culture flasks, plates, dishes	Disposable cell culture material	TPP Trasadigen, Switzerland
Curix 60	Tabletop film processor	Agfa Cologne, Germany
Cyclone	Storage Phosphor Screens	Canberra-Packard Schwadorf, Austria
FACSCalibur	Flow cytometer	Becton Dickinson Heidelberg, Germany
IBIDI™ μ -slide	Microscope slide	IBIDI GmbH Munich, Germany
LSM 510 Meta	Confocal laser scanning microscope	Zeiss Jena, Germany
Mikro 22R	Table centrifuge	Hettich Tuttlingen, Germany
Nanodrop® ND-1000	Spectrophotometer	Peqlab Wilmington, DE, USA
Nucleofector II	Electroporation device	Lonza GmbH Cologne, Germany
Odyssey 2.1	Infrared Imaging System	LI-COR Biosciences Lincoln, NE USA
Orion II Microplate Luminometer	Luminescence	Berthold Detection Systems Pforzheim, Germany
Polytron PT1200	Ultrax homogenizer	Kinematica AG Lucerne, Switzerland
SpectraFluor Plus™	Microplate multifunction reader	Tecan Männedorf, Austria
Sunrise™	Microplate absorbance reader	Tecan Männedorf, Austria
Vi-Cell™ XR	Cell viability analyzer	Beckman Coulter Fullerton, CA, USA

3.2 Methods

3.2.1 Cell Culture

3.2.1.1 Cell lines: Skbr3 and L3.6pl

The human breast cancer cell line Skbr3 cells were a kind gift from Barbara Mayer (Department of Surgery, Klinikum Grosshadern, LMU Munich) and cultured with McCoy's (PAA Laboratories, Coelbe, Germany), supplemented with 10% heat-inactivated FCS gold (Biochrom AG, Berlin, Germany).

The human pancreatic cancer cell line L3.6pl was generously provided by Christiane J. Bruns (Department of Surgery, Klinikum Grosshadern, LMU Munich) and cultured (37°C and 5% CO₂) on Collagen G coated culture flasks with DMEM, supplemented with 10% heat inactivated FCS gold, 1x NEAA and 1 mM pyruvate.

3.2.1.2 Cultivation of cell lines

Cell lines were incubated at 37°C with 5% CO₂ in a humidified incubator. The cells were cultivated as monolayers and split upon reaching 80% to 90% confluence.

To split the cell lines, cells were rinsed one time using PBS and detached from the cell culture flasks using Trypsin/EDTA (T/E). The T/E reaction was stopped by adding growth medium to the cells and removed by centrifugation (1000 RPM, 5 minutes, room temperature). Cells were resuspended in fresh medium and split 1:5 for further cultivation or used for experiments.

3.2.1.3 Freezing, thawing and long term storage

To ensure similar experimental results, all cell lines were passaged no more than 10 times before discarding and thawing a fresh stock.

To freeze-back the cell lines, cells were harvested with T/E and resuspended in freezing medium (70% relative growth medium, 20% FCS, 10% DMSO) at a concentration of 2.0×10^6 cells/ml and initially frozen in cryovials at -20°C for 24 hours, and thereafter transferred to -80°C for short term storage or into liquid nitrogen for long term storage. The individual cryovials were rapidly thawed to room temperature and suspended in growth medium to reduce the amount of exposure to DMSO upon thawing. Cells were washed and centrifuged (1000 RPM, 5 minutes,

room temperature) before resuspending them in growth medium. Then they were cultivated for at least three days before splitting them for use in experiments.

3.2.2 Flow cytometry

Flow cytometry (FCM) is a technique used to count and examine microscopic particles, such as cells labeled with fluorescent tagged antibodies or stains (e.g. propidium iodide), by suspending them in a thin stream of fluid and passing them by an electronic detection apparatus. This technique allows simultaneous multi-parametric analysis of the physical or chemical characteristics of thousands of particles per second. Based on these parameters, fluorescent-tagged antibodies or various stains can be utilized to measure apoptosis, cell cycle or expression and localization of antigens.

3.2.2.1 Apoptosis analysis

Quantification of apoptosis was performed according to Nicoletti et. al.⁸⁵ Briefly, 1.5×10^5 L3.6pl or Skbr3 cells were seeded per well into 24-well plates and allowed to adhere overnight. Growth medium was exchanged and cells were stimulated with desired substances for 24 or 48 hours, respectively. Cells were washed, trypsinized and resuspended before centrifugation for 10 minutes $600 \times g$ at $4^\circ C$. Samples were washed with PBS to remove remaining debris, centrifuged and resuspended in HFS buffer containing 2 mg/ml propidium iodide (PI). Stained cells were protected from light and incubated for at least 2 hours at $4^\circ C$. PI stained cells were detected by flow cytometry.

Table 6. Buffers for FCM analysis

HFS Buffer		FCM Buffer	
Na ₃ -citrate 0.1%	0.10%	NaCl	8.12 g
Triton-X 100 0.1%	0.10%	KH ₂ PO ₄	0.26 g
PBS	1 mL	Na ₂ HPO ₄	2.35 g
		KCl	0.28 g
		Na ₂ EDTA	0.36 g
		LiCl	0.43 g
		Na-azide	0.20 g
		H ₂ O	to 1 L, pH 7.4

3.2.2.2 Anoikis analysis

Anoikis is a type of cell death that occurs when anchorage-dependent cells detach from the ECM. Anchorage-dependent cells remain adherent to the tissue to which they belong, allowing for communication between neighboring cells which provide essential growth or survival signals. Following cell-detachment from the ECM, cell-matrix interactions are disrupted, typically resulting in anoikis. However, metastatic tumor cells evade anoikis induction to invade other tissues.

Cell lines were prevented from adhering to the bottom of culture wells by culturing them in 24-well plates coated with polyHEMA as described by Bourguignon et al.⁸⁶ Briefly, cultures were trypsinized and plated at 0.75×10^5 cells per well onto 24-well polyHEMA-coated plates. PolyHEMA-coated plates contained 0.3 ml of 10 mg/ml solution of polyHEMA/ethanol per well and were dried overnight in the tissue culture hood. After appropriate time periods of growth in forced suspension, cells were harvested for apoptosis detection as described under section 3.2.2.1.

3.2.2.3 Cell cycle analysis

To analyze the cell cycle, the fluorescence intensity was measured in the logarithmic mode of the fluorescence channel 2 (FL2, λ_{em} 585 nm) using a flow cytometer. Cells are treated using propidium iodide which intercalates into the DNA-helix, the output of its fluorescence depends on the status of cellular chromatin.

In the control cells, most of the cells are in the G0/G1 cell cycle phase with 2n chromosome set, lacking the sister chromatids. Cells found in the G2/M-phase are in the process of dividing, containing both the normal 2n chromosome set in addition to the duplicate sister chromatids. The duplication of chromatids allows for the G2/M-phase to be differentiated from the G0/G1-phase due to the higher fluorescence peak caused by the increased propidium iodide intercalation. Cells in the S-phase are undergoing synthesis wherein the chromatids are duplicated. The fluorescence peak of cells in the S-phase is found between the fluorescence peaks of G0/G1- and G2/M-phase. Finally in apoptotic cells, DNA is fragmented which generates a peak which is found to the left of the G0/G1 fluorescence. During graphical analysis, regions were gated for each fluorescence peak of the four enumerated chromatin states, and cells of each region were quantified using the Cell QuestTM software or by utilizing the cell cycle analysis program FlowJoTM.

3.2.2.4 β 1 Integrin surface expression

Surface expression of β 1 integrin was measured using FCM analysis. 0.80×10^5 Skbr3 cells were seeded and allowed to adhere for 8 hours before stimulation with 6BIO for 30 minutes to 24 hours. Thereafter cells were harvested with Trypsin/EDTA (T/E) and washed one time with PBS before blocking with 2% BSA for 15 minutes at room temperature. Cells were incubated with the primary anti- β 1 integrin antibody (Santa Cruz) for one hour at room temperature, washed one time with PBS and incubated with Alexa Fluor 488 goat-anti-mouse antibody (Molecular Signaling/Invitrogen) for 30 minutes at room temperature protected from light. Cells were washed one final time to remove unbound secondary antibody and re-suspended in PBS containing 0.5% BSA and the fluorescence was read at 488 nm in the FACS machine immediately.

3.2.3 Cell viability measurements

The viability of cells was measured with the VI-CELL™ cell viability analyzer (Beckman Coulter, Krefeld, Germany) after exposure to 6BIO for 24 or 48 hours. Briefly, 1.5×10^5 Skbr3 cells were seeded in 24-well plates and allowed to adhere overnight before stimulating with 6BIO for 24 hours. Cells were harvested with T/E, resuspended in growth medium and read immediately in the VI-CELL™.

3.2.4 Proliferation

1.5×10^3 Skbr3 or L3.6pl cells were seeded per well into 96-well plates. The next day, control cells were fixed and stained with crystal violet to determine the initial cell number. Then cells were treated with increasing concentrations of 6BIO or 7BIO for 72 hours. After stimulation, cells were stained with crystal violet solution (0.5% crystal violet in 20% methanol) for 10 minutes. Unbound crystal violet was removed by rinsing with distilled water and cells were subsequently air-dried. Next, crystal violet which mainly binds to DNA was eluted from the cells with 0.1M sodium citrate in 50% ethanol. The absorbance of crystal violet is proportional to the cell number and was determined with the Sunrise ELISA reader (Tecan Trading AG, Maennedorf, Switzerland) at 550 nm.

3.2.5 Migration and invasion

3.2.5.1 Wound healing assay

1.5×10^5 Skbr3 or L3.6pl cells were seeded into 24-well plates and grown to confluence. A wound of approximately 1 mm was inflicted to each cell monolayer by scratching them with a yellow pipet tip. One PBS wash removed the detached cells before incubation for 16 hours at 37°C in either starvation medium (McCoys) or growth medium or growth medium with increasing concentrations of 6BIO. After incubation, cells were washed with PBS and fixed with 4% formaldehyde. One image per well was taken using an inverted light microscope using the Imago_QE camera system and the appending software (Till Photonics, Graefelfing, Germany). For quantification, these images were analyzed with S.CORE imaging analysis tool (S.CO LifeScience, Munich, Germany). This software tool identifies the cell covered area by using an algorithm based on brightness and contrast values. The cell-free area correlates to the ability of the cells to migrate into the wound.

3.2.5.2 Migration through membranes

Cellular migration through a 6.5 mm diameter tissue culture-treated polycarbonate membrane with 8 μM pores was assessed as follows: 1.0×10^5 cells were placed in the upper chamber of a Transwell™ unit containing serum-free medium with or without 6BIO. The lower chamber was pre-coated with collagen G and contained growth medium. Plates and inserts were incubated for 24 hours at 37°C (L3.6pl) or prestimulated with 6BIO for 20 hours and seeded into inserts for 4 hours (Skbr3). Transwell™ inserts were removed and stained with crystal violet. The cells that did not migrate from the upper chamber to the lower chamber were removed using a cotton swab and images were taken from each insert before the incorporated dye from the migratory cells was extracted with a 1:1 solution of 0.1M sodium citrate and 50% ethanol. The absorbance was measured at 550 nm in the Sunrise ELISA plate reader (Tecan Trading AG, Maennedorf, Switzerland).

3.2.5.3 Chemotaxis assay

Chemotaxis of 6BIO-treated Skbr3 cells was investigated by the IBIDI™ μ -slide (IBIDI, Martinsried, Germany). The chemotaxis assay was performed as described by the manufacturer. As seen in Figure 3.1, a Skbr3 suspension (7 μ l) of 5.0×10^6 cells/ml was seeded into the center chamber of a μ -slide. The opposing medium reservoirs were filled with starvation medium and culture medium containing 10% FCS, respectively. The FCS diffuses linearly and in a stable manner, allowing for an FCS gradient from 0 to 10% in the seeding chamber of the μ -slide.

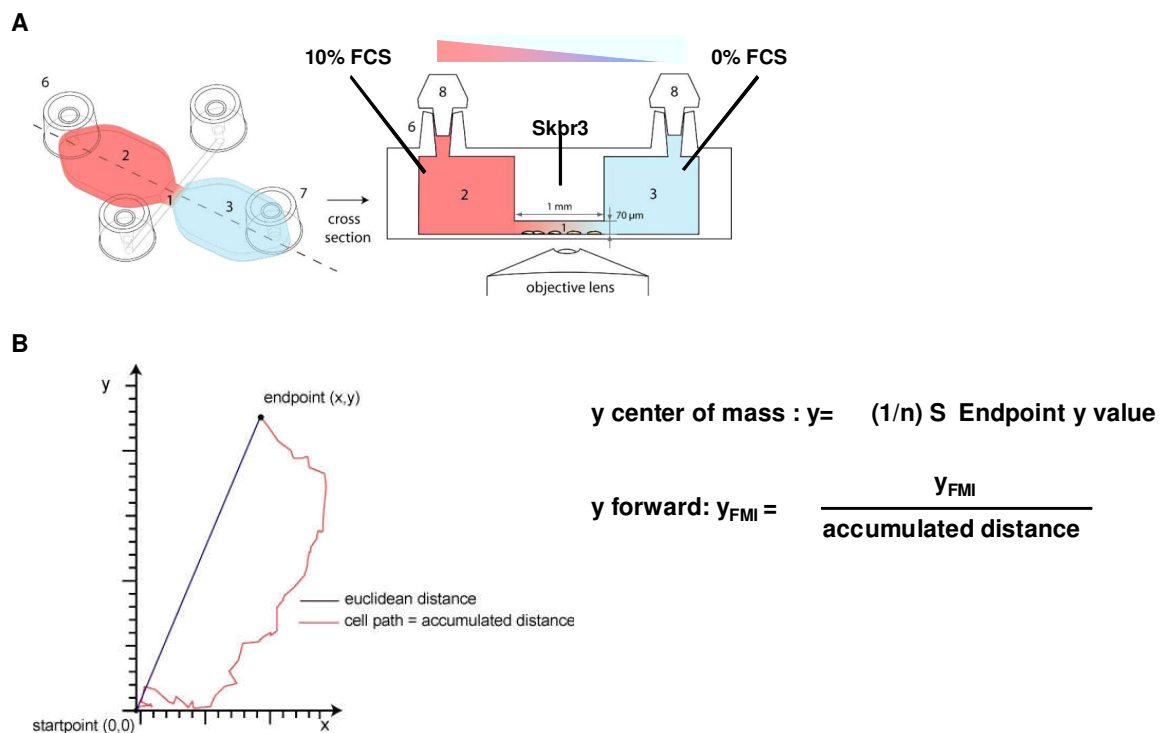


Figure 3.1: Chemotaxis assay in an IBIDI™ μ -slide

Images are taken from the IBIDI chemotaxis protocol:
 (A) Pictorial representation of the chemotaxis assay.
 (B) Graphical representation of cellular movements.

Cell movement was recorded every 10 minutes over 24-hours by live cell imaging in a cell observation chamber (IBIDI) on the inverted light microscope using the Imago-QE camera system and Till photonics software. Cell tracking and analysis were done using the manual tracking plug-in (Fabrice Cordelieres, Orsay, France) and the chemotaxis and migration tool (IBIDI) for ImageJ (US National Institutes of Health, Bethesda, MD, USA), as described in the μ -slide chemotaxis protocol. The position of cells was defined as a point at low magnification from a 10x lens.

3.2.5.4 Matrigel™ invasion assay

Cellular invasion was measured using 6.5 mm diameter tissue culture-treated polycarbonate membrane with 8 μM pores (Costar). Membranes were coated with a 1:2 dilution of Matrigel™ in medium according to manufacturer's instructions.

1.0×10^5 cells were placed in the upper chamber of the Transwell™ unit containing serum-free medium with or without 6BIO and lower chambers containing growth medium and fibronectin as an attractant. Skbr3 cells were allowed to invade for 20 hours at 37°C. Transwell™ inserts were removed and stained with crystal violet. The cells that did not migrate from the upper chamber to the lower chamber were removed using a cotton swab and images were taken from each insert before the incorporated dye from the migratory cells was extracted with a 1:1 solution of 0.1M sodium citrate and 50% ethanol and the absorbance was measured at 550 nm in the Sunrise ELISA plate reader. Each assay was set up in duplicate and repeated at least three times. Images of invaded cells were analyzed using ImageJ software.

3.2.6 Cell adhesion on fibronectin

Cell adhesion was examined in 24-well plates coated with fibronectin. 1.0×10^5 Skbr3 cells/well were allowed to adhere for 1.5 hours at 37°C. Wells were washed with PBS to remove any unbound cells and stained with crystal violet. Incorporated dye was extracted with a 1:1 solution of 0.1M sodium citrate and 50% ethanol and the absorbance was measured at 550 nm in the Sunrise™ ELISA plate reader.

3.2.7 Western blot

3.2.7.1 Sample preparation

For Western blot analysis, cell samples were washed 2x with ice-cold PBS following stimulation and were lysed by adding RIPA buffer to each sample well and frozen at -80°C. Next, cells were thawed on ice, and contents of triplicate wells were pooled into 1.5 ml reaction tubes. To remove all cellular debris, tubes were centrifuged for 10 minutes at 10,000x g at 4°C. Supernatants were carefully transferred to a new reaction tube, and aliquots were taken for protein quantification (see 3.2.7.3).

5x SDS-sample buffer was added to the lysates, mixed gently and boiled at 95°C for 5 minutes. All samples were stored at -20°C when not in use.

Table 7. Buffers for preparation of total cell lysates

RIPA Buffer		5x SDS-Sample Buffer	
Tris/HCl	0.79 g	Tris/HCl	3.13 M pH 6.8
NaCl	0.87 g	Glycerol	10 mL
Nonidet NP 40	1.0 mL	SDS	5.00%
Deoxycholic acid	0.25 g	DTT	2.00%
SDS	0.10 g	Pryonin Y	0.03%
Complete®	1:25	H ₂ O	to 20 mL
PMSF	1.0 mM		
Na ₃ VO ₄	1.0 mM		
NaF	1.0 mM		
H ₂ O	to 100 mL		

3.2.7.2 Immunoprecipitation

For evaluation of Rac1 levels, pull-down assays were performed using the Rac1/Cdc42 Activation Assay Kit 89856 (Pierce, Rockford, IL). Briefly, 1.0×10^5 Skbr3 cells were seeded in triplicate into 24-well plates pre-coated with fibronectin and allowed to adhere for 1 hour. Cells were harvested with lysis buffer, pooled together and incubated with a Rhotekin RDB agarose slurry or GST human Pak1-PDB for 1 hour at 4°C respectively. Samples were thoroughly washed and proteins were detected using Western blot analysis. Adjustment of the protein contents of respective samples was controlled by a Bradford-assay (see 3.2.7.3) prior to each Western blot. ImageJ (US National Institutes of Health, Bethesda, MD, USA) was used to quantify bands.

3.2.7.3 Protein quantification

Protein samples were quantified according to Bradford et al.⁸⁷ The standard calibration curve was generated using samples containing defined concentrations of BSA suspended in H₂O (50 µg/ml – 500 µg/ml). 190 µl of the Bradford reagent (Bradford reagent stock was diluted 1:5 in H₂O) was added to each 10 µl aliquot of diluted protein samples (diluted 1:10 in H₂O) and calibration samples in a 96-well flat bottom plate. All measurements were performed in duplicate. Probes were incubated for 5-10 minutes and the absorbance was measured in the Sunrise™ ELISA reader.

3.2.7.4 SDS-PAGE

SDS-PAGE according to Laemmli⁸⁸ was performed by using the Mini Protean III system from Bio-Rad (Munich, Germany). Prior to loading the samples, the apparatus was assembled as described by the producer, and the chamber filled with chilled electrophoresis buffer. Equal protein concentrations of samples were loaded onto the SDS-gel and any empty slots were filled with an equal volume of 1x SDS-sample buffer. 1.5 μ L of the Fermentas Page RulerTM Prestained Protein Ladder was loaded on each gel to estimate the molecular weights of the separated proteins.

Table 8. Buffers and gels for Western blotting

Electrophoresis buffer	
Tris base	3.0 g
Glycine	14.4 g
SDS	1.0 g
H ₂ O	to 1.0 L

Stacking gel		Separating gel	
30 % PAA solution	1.28 mL	30 % PAA solution	5.0 mL
1.25 M Tris/Hcl pH 6.8	0.75 mL	1.25 M Tris/Hcl pH 6.8	3.75 mL
10 % SDS	75 μ L	10 % SDS	150 μ L
H ₂ O	5.25 mL	H ₂ O	6.1 mL
APS	75 μ L	APS	75 μ L
TEMED	20 μ L	TEMED	20 μ L

3.2.7.5 Tank blotting

After separating the proteins on a gel in the SDS-PAGE, proteins were transferred to a nitrocellulose membrane (Hybond-ECLTM, Amersham Bioscience, Freiburg, Germany) via standard tank blotting. A blotting sandwich was prepared in a box filled with 1x tank buffer to avoid bubbles as described by the producer. Prior to running the blot, all pads, papers, and membranes were equilibrated with 1x Tank buffer for at least 10 minutes. Membrane sandwiches were mounted in the Mini Trans-Blot[®] system (Bio-Rad, Munich, Germany). Ice-cold 1x Tank buffer was filled into the chamber and an ice pack was inserted to avoid excessive heat. Tank blots were carried out at 4 °C, either at 100 V for 90 minutes or at 23 V overnight.

Table 9. Tank buffer

5x Tank buffer		1x Tank buffer	
Tris base	15.2 g	5x Tank buffer	200 mL
Glycine	79.2 g	Methanol	200 mL
H ₂ O	to 1.0 L	H ₂ O	to 1.0 L

3.2.7.6 Detection

Following the transfer, gels were stained in a Coomassie solution, and all membranes were washed once in TBS-T. Membranes were incubated in 5% Blotto or BSA to block unspecific binding followed by an overnight incubation period at 4°C with the primary antibody dilution (Table 10). To remove all unbound primary antibody, all membranes were washed 4x in TBS-T prior to incubation for 1 hour protected from light at room temperature with the secondary antibody dilution (Table 11).

Either of two detection methods was utilized to develop the membranes as described below:

Detection method – LICOR: Secondary antibodies coupled to IRDyeT^M 800 and Alexa Fluor® 680 with emission at 800 and 700 nm, respectively, were used. Membranes were incubated for 1 hour. Protein bands of interest were detected using the Odyssey imaging system (LICOR Biosciences, Lincoln, NE). Secondary antibodies used for this type of protein detection are listed in Table 11. After washing, membranes were scanned and analyzed, and proteins were quantified using the ImageJ gel analyzer plugin.

Detection method – Enhanced Chemiluminescence: Membranes were incubated for 2 hours with HRP-conjugated secondary antibodies (Table 11). For detection, luminol was used as a substrate. The membrane was incubated with ECL (enhanced chemiluminescence) solution for 1 minute (ECL Plus Western Blotting Detection Reagent RPN 2132, GE Healthcare, Munich, Germany). The appearing luminescence was detected by exposure of the membrane to an X-ray film (Super RX, Fuji, Düsseldorf, Germany) and subsequently developed with a Curix 60 Developing system (Agfa-Gevaert AG, Cologne, Germany).

Table 10. Primary antibodies

Antigen	Source	Dilution	In	Provider
β -actin	Mouse monocl.	1:1,000	Blotto 1%	Chemicon
Akt	Rabbit polycl.	1:1,000	BSA 5%	Cell Signaling
phos.-Akt ^{S473}	Mouse IgG2b	1:1,000	Blotto 5%	Cell Signaling
phos.-Akt ^{T308}	Rabbit IgG	1:1,000	BSA 5%	Cell Signaling
β 1 integrin	Rabbit polycl.	1:1,000	Blotto 5%	Cell Signaling
phos- β 1 Integrin ^{S785}	Rabbit polycl.	1:500	BSA 5%	Gen Way/Biozol
phos.-ERK ^{T202/Y204}	Rabbit polycl.	1:1,000	BSA 5%	Cell Signaling
FAK	Mouse monocl.	1:1,000	BSA 5%	Santa Cruz
phos.-FAK ^{T397}	Rabbit polycl.	1:500	BSA 5%	Santa Cruz
PI3K (p85)	Rabbit polycl.	1:1,000	BSA 5%	Upstate
Rac1	Mouse monocl.	1:1,000	Blotto 5%	Upstate

Table 11. Secondary antibodies

Antibody	Dilution	In	Provider
Goat anti-mouse IgG1: HRP	1:1,000	Blotto 1%	Biozol
Goat anti mouse IgG: HRP	1:1,000	Blotto 1%	Southern Biotech
Goat anti-rabbit: HRP	1:1,000	Blotto 1%	DiANOVA
Alexa Fluor [®] 680 Goat-anti-mouse IgG	1:10,000	Blotto 1%	Molecular Probes
Alexa Fluor [®] 680 Goat-anti-rabbit IgG	1:10,000	Blotto 1%	Molecular Probes
IRDye [™] 800CW Goat-anti-mouse IgG	1:20,000	Blotto 1%	LI-COR
IRDye [™] 800CW Goat-anti-rabbit IgG	1:20,000	Blotto 1%	LI-COR

3.2.7.7 Staining of gels and membranes

Gels were stained for 30 minutes in the Coomassie staining solution and destained with the Coomassie destaining solution to control equal loading of the gel and the performance of the transfer. A 0.2% Ponceau S in 5.0% acetic acid solution was used to stain membranes. Destaining was performed in distilled water.

Table 12. Gel staining solution

Coomassie Staining Solution		Coomassie Destaining Solution	
Coomassie blue	3.0 g	Glacial acetic acid	100 mL
Glacial acetic acid	100 mL	Ethanol	333 mL
Ethanol	450 mL	H ₂ O	to 1 L
H ₂ O	to 1 L		

3.2.8 Confocal laser scanning microscopy (CSLM)

Cell imaging was assessed by seeding $0.2 - 1.0 \times 10^5$ Skbr3 cells in 8-well chamber glass sides (IBIDI) followed by stimulation with various concentrations of 6BIO for 30 minutes to 24 hours. After three PBS washing steps, cells were fixed with 4% paraformaldehyde in PBS for 15 minutes at room temperature followed by permeabilization by incubating with .2% Triton X-100 in PBS for 2 minutes. Cells were blocked with 0.2% bovine serum albumin (BSA) and incubated with specific antibodies against Akt (Cell Signaling), pT308 Akt and pS473 Akt (Cell Signaling), Rac1 (Upstate), integrin β 1 (Cell Signaling), pS785 integrin β 1 (GenWay), FAK (Santa Cruz), and pT397 FAK for 1 hour. Specific proteins were visualized by secondary antibodies [Alexa Fluor 633-linked goat anti-mouse (Invitrogen) and Alexa Fluor 488-linked goat anti-rabbit (Invitrogen)]. Rhodamine phalloidin was used for F actin staining. PermaFluorTM mounting medium and individual coverslips were placed over each well for confocal microscopy. Split channel images were taken by Zeiss Meta confocal laser scanning microscopy (CSLM) with the 40x oil immersion lens.

3.2.9 Skbr3 and fibroblast spheroids

Spheroids are an important tool to evaluate the drug efficacy in that is well supported that they resemble real tissues more closely in structure and in functional properties.⁸⁹

3.2.9.1 Metabolic inhibition of Skbr3 spheroids

In close collaboration with Dr. Barbara Mayer (SpheroTec, Martinsried, Germany), homotypic spheroids consisting either of Skbr3 tumor cells or fibroblasts were prepared according to the methodology of SpheroTec. Briefly, 96-well plates were coated with polyHEMA (Sigma Aldrich, Dreieich, Germany) to prevent attachment

of the tumor cells to the plastic dish. Multi-cellular spheroids were initiated from monolayer cultures treated with 1mM EDTA (Sigma), pH 7.2 at 37°C to prepare single-cell suspensions. After washing twice, cell viability was determined using the trypan blue exclusion test, and 5×10^4 viable cells in 100 μ l cell culture medium supplemented with 10% FCS, 2% vitamine and 2% NEAA were plated in each well. This procedure resulted in a single multicellular spheroid per well.

Orthotopic fibroblasts were prepared from human breast cancer samples by culturing minced tissue in DMEM/F12 medium supplemented with 10% FCS, 2% vitamin and 2% NEAA. Fibroblasts were cell-typed and used in early passages up to passage number 8. All cell culture products were purchased from PAN (Aidenbach, Germany).

Mature Skbr3 spheroids were then examined over a 93- and a 165-hours period in individual wells of a 96-well plate in growth medium with or without increasing doses of 6BIO. Spheroids were then individually photographed before the addition of MTT/PMS (MTT: 2 mg/ml, PMS: 0.92 mg/ml). After 6 hours at 37°C in a humidified 5% CO₂ atmosphere, the absorbance at 490 nm (reference wavelength 650 nm) was measured with a 96-well plate ELISA reader (Tecan, Crailsheim, Germany). Three replicates per treatment were performed.

3.2.9.2 Skbr3 spheroid confrontation with fibroblast spheroids

The Skbr3 and fibroblast spheroids were cultivated as described above. Thereafter, individual spheroids of each type were confronted in individual wells containing growth medium with or without increasing doses of 6BIO for 48 hours. The degree of migration in the absence and presence of 6BIO was captured over time by microscopy (Zeiss, Jena, Germany).

3.2.10 Statistical analysis

All experiments were performed at least three times in triplicate unless otherwise noted. Results are expressed as mean value \pm SEM. One-way ANOVA with Turkey post-tests or individual Students t-tests were performed using SigmaStat version 3.5 for Windows or GraphPad PrismTM. P-values < 0.05 were considered significant.

4 RESULTS

4.1 Antitumor effects of 6BIO and 7BIO *in vitro*

Based on the promising preliminary results of the indirubin derivatives in the kinase assays by Zahler et al.¹¹ we investigated the basic antitumor properties of 6BIO and 7BIO in a variety of *in vitro* systems using the highly invasive breast cancer cell line Skbr3 and the pancreatic cell line L3.6pl.

4.1.1 Effects of 6BIO and 7BIO on apoptosis

The effects of 6BIO and 7BIO were assessed for the induction of apoptosis and on the cell cycle using flow cytometry. Tumor cells were stimulated with increasing doses of both substances and significant apoptosis was induced starting with 10 μM 6BIO (approximately 39% Skbr3, 33% L3.6pl) and at least 30 μM 7BIO (approximately 38% Skbr3, 24% L3.6pl) for both cell lines (Figure 4.1).

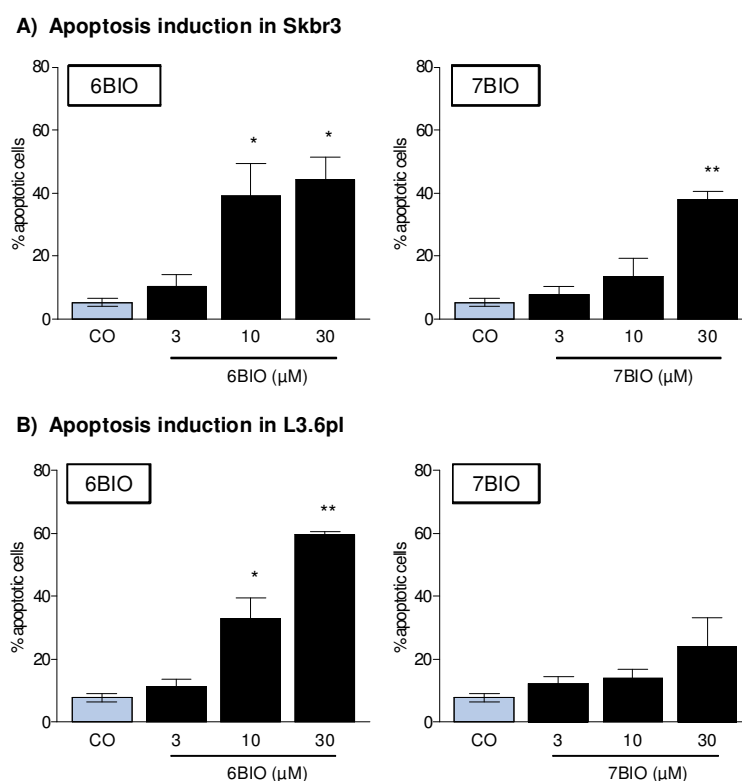


Figure 4.1: Induction of apoptosis by indirubin derivatives

Skbr3 (A) and L3.6pl (B) cells were seeded and allowed to adhere overnight before stimulation with increasing doses of BIO's for 48 or 24-hours, respectively. One-way ANOVA/Turkey tests were used to assess significance. Bars represent \pm SEM from three independent experiments performed in triplicate. *, $P < 0.05$ **, $P < 0.001$.

4.1.2 Effects of 6BIO and 7BIO on anoikis induction

Next, anoikis levels (or otherwise defined as levels of programmed cell death caused by anchorage independence) were similarly assessed via FCM analysis using PI staining as described in Materials and Methods.

6BIO treatment and 7BIO treatment caused significantly varied effects in both cells lines. Skbr3 cells treated with 6BIO did not vary from controls with the exception of the 24-hour time point which showed a slight, but not significant reduction of anoikis (~12%) in comparison to the controls (~21%) (Figure 4.2). Skbr3 cells treated with 7BIO showed no variance in anoikis induction until the 24-hour time point, where it slightly (~29%), but not significantly induced the amount anoikis (Figure 4.2A).

L3.6pl cells treated with 6BIO showed increased anoikis after 8 hours (~12%) vs. control cells (~4%) and more significantly at 12 hours (~33% vs. control ~17%). 7BIO treatment of L3.6pl also induced significant anoikis beginning at the 8-hour time point (~12% vs. control ~4%) and showing an even greater difference at 12 hours (~29% vs. control ~17%) as seen in Figure 4.2B.

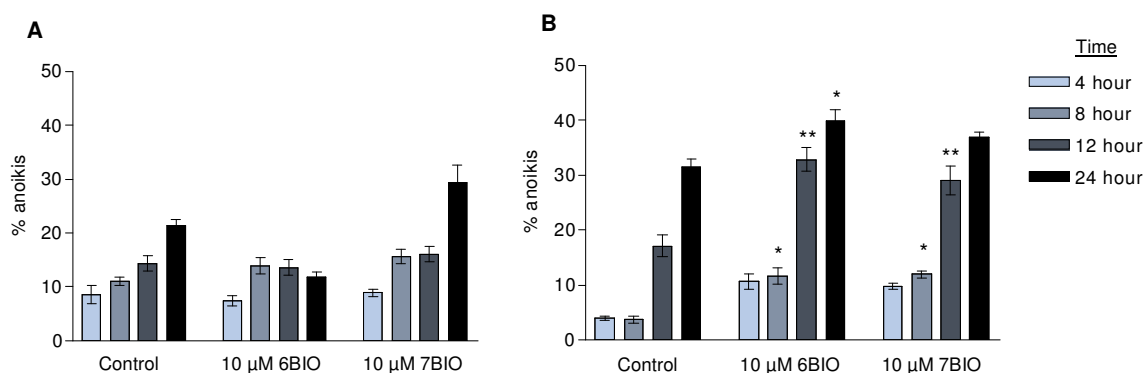


Figure 4.2: Mild anoikis-inducing effects of 6BIO and 7BIO

Skbr3 (A) and L3.6pl (B) cells were seeded into polyHEMA coated 24-well plates as defined in Materials and Methods and stimulated with 10 μM of 6BIO or 7BIO or left untreated (Control) for up to 24 hours. One-way ANOVA/Turkey tests were used to assess significance. Bars are the SEM of three independent experiments performed in triplicate with *, $P < 0.05$ and **, $P < 0.001$.

4.1.3 Effects on tumor cell proliferation by 6BIO and 7BIO treatment

Proliferation of both cell lines was significantly affected by treating the cells with the indirubin derivatives in comparison to the controls. Proliferation was assessed using crystal violet staining as described in Materials and Methods. It was dose-dependently inhibited by increasing concentrations of both substances (Figure 4.3).

Skbr3 cells (Figure 4.3A) treated with 6BIO showed a 76% (10 μ M 6BIO) and a 86% (30 μ M 6BIO) as well as 57% (10 μ M 7BIO) and an 84% (30 μ M 7BIO) average decrease in proliferation in comparison to control wells.

L3.6pl cells were affected at even lower doses, namely 50% at 1 μ M, 70% at 3 μ M and 78% at 10 μ M 6BIO, as well as 55 % at 1 μ M and approximately 76% at both 3 and 10 μ M 7BIO (Figure 4.3B).

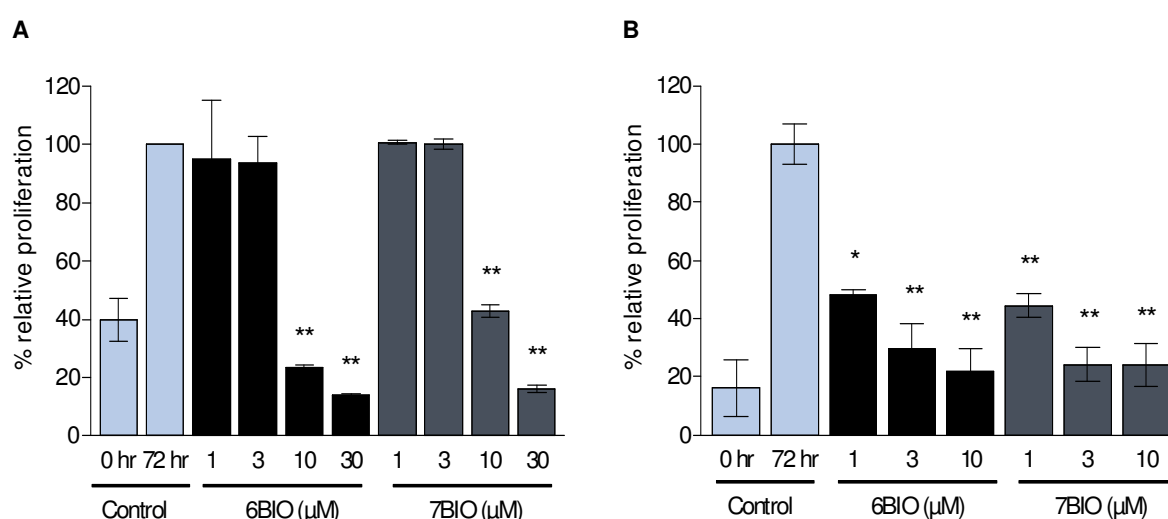


Figure 4.3: Reduced tumor cell proliferation by BIO's in a dose-dependent manner

Skbr3 (A) and L3.6pl (B) cells were allowed to adhere for 24-hours prior to stimulation of cells with increasing doses of BIO's or left untreated (Control). Cells were stained with crystal violet as described in Materials and Methods and the absorbance was calculated relative to the control wells. One-way ANOVA/Turkey tests were used to assess significance. Bars are the SEM of three independent experiments performed in triplicate with *, $P < 0.05$ and **, $P < 0.001$.

4.1.4 Effects of 6BIO on cell viability in Skbr3 breast cancer cells

Skbr3 cells were seeded and allowed to adhere before stimulation with increasing doses of 6BIO and determination of cellular viability in the VI-CELL™. Cellular viability was decreased with increasing concentrations of 6BIO (Figure 4.4). Reduction of Skbr3 viability was obvious beginning with 10 μM 6BIO (39% viable cells), and significant at 25 μM 6BIO treatment (72% viable cells) as well as highly significant at 50 μM 6BIO treatment (29% viable cells).

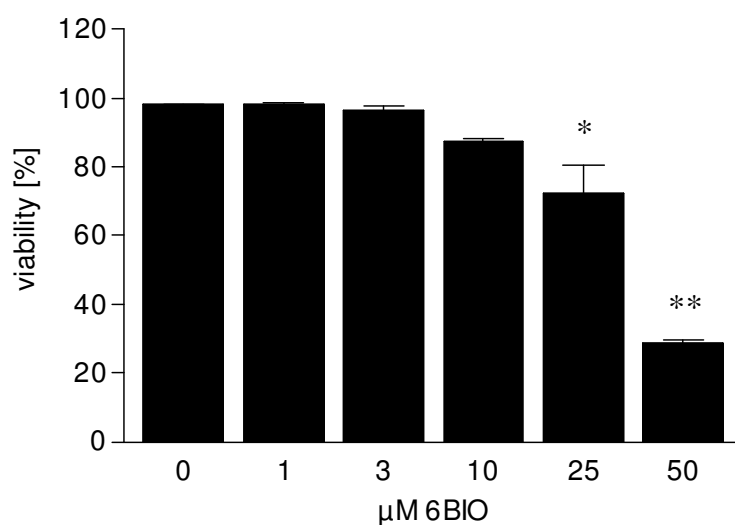


Figure 4.4: Significant effect on cellular viability by treatment with 6BIO

Skbr3 cells were seeded and allowed to adhere before 24-hours of stimulation with increasing doses of 6BIO. Cells were harvested and measured using a VI-CELL™. One-way ANOVA/Turkey tests were used to assess significance. Bars are the SEM of three independent experiments performed in triplicate with *, $P < 0.05$ and **, $P < 0.001$.

4.1.5 Breakdown of cell cycle upon 6BIO treatment

In order to understand the mechanism by which the 6BIO affects the cell growth, the cell cycle breakdown was analyzed. The cell cycle is composed of 4 distinct phases; G1 phase, S phase (synthesis), G2 phase (interphase) and M phase (mitosis). The DNA content of the cell varies upon which phase it is in, namely G1/G0 which have a haploid DNA content and G2 shows a diploid DNA content. Treatment with 6BIO arrested the cell in the S phase in Skbr3 cells and in the S phase/G2 phase for L3.6pl cells as seen in Figure 4.5.

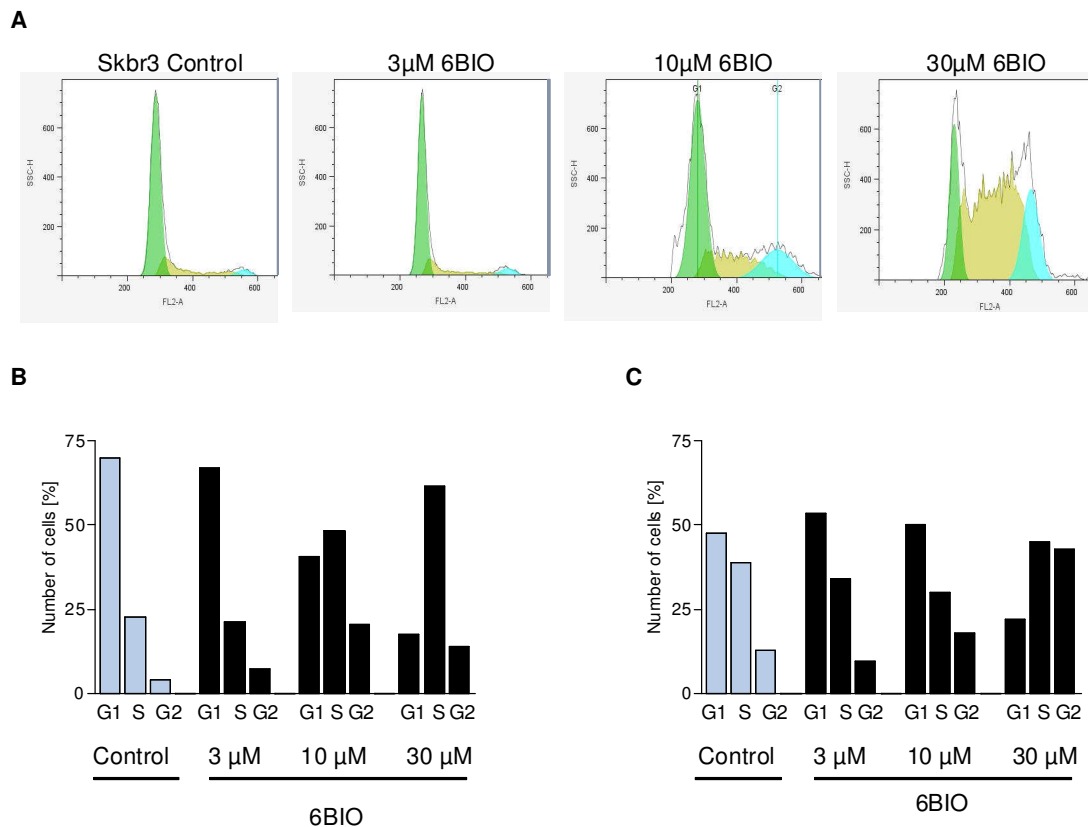


Figure 4.5: Effect of 6BIO treatment on the cell cycle

Both cell lines were allowed to adhere overnight before stimulation with increasing doses of 6BIO or left as untreated controls (Control). Upper panels from Skbr3 (A) show an example set of histogram from the cell cycle distribution as quantified by the FlowJo™. Lower panels from Skbr3 (B) and L3.6pl (C) show a graphical representation of the cell cycle breakdown from at least one data set. Experiments were performed three times in triplicate.

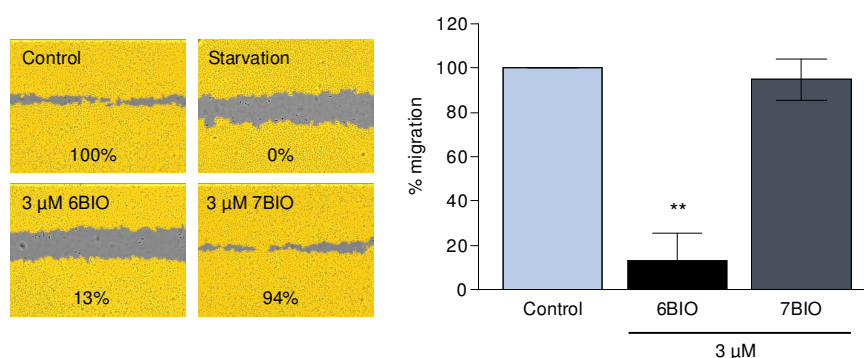
Taken together, 6BIO and 7BIO show dose- and time-dependent antitumor activity through the induction of apoptosis and their effects on the cell cycle. Furthermore, they reduced both proliferation and viability of the tumor cells

4.2 Different effects of 6BIO and 7BIO on metastatic pathways

4.2.1 Impairment of wound healing by 6BIO treatment

To initially assess the potential anti-migratory effects of the indirubin derivatives, wound healing assays were performed as outlined in Materials and Methods. 3 μM of both substances was selected as the dose to treat the cells with as this was a concentration low enough in both cells lines to have little to no effect on apoptosis or the cell cycle. Interestingly, 6BIO but not 7BIO significantly reduced the migration of both cell lines into the wounds. 6BIO reduced Skbr3 migration to about 13% of the control, whereas 7BIO allowed still 94% migration with respect to the control. (Figure 4.6A). L3.6pl cells were equally affected; with 6BIO treatment allowing for only 41% migration and 7BIO treatment for 86% respectively (Figure 4.6B).

A Wound healing assay in Skbr3 cells



B Wound healing assay in L3.6pl cells

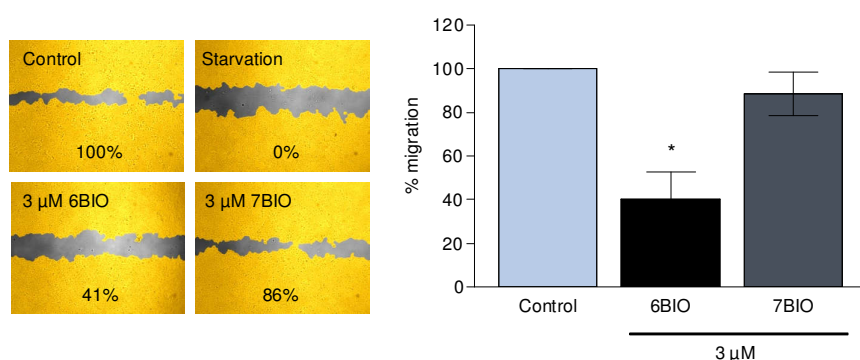


Figure 4.6: Disruption of the wound closure ability by 6BIO

Images on left: Representative images from triplicate experiments. Both cell lines were seeded and allowed to adhere as a confluent monolayer. This monolayer was wounded and treated with 3 μM 6BIO or 7BIO or left untreated and allowed to close the wound for 16 hours (Skbr3) or 20 hours (L3.6pl). The cell covered area is shown in yellow, whereas gray indicates uncovered area.

Graphs on right: The quantification is expressed as the percent migration related to untreated cells (control, 100%). One-way ANOVA/Turkey tests were used to assess significance. Bars are the SEM of three independent experiments performed in triplicate with *, $P < 0.05$ and **, $P < 0.001$.

4.2.2 Effect of 6BIO on migration through Transwell™ inserts

As 6BIO but not 7BIO was able to disrupt wound closure, its ability to block directed migration in response to chemoattractants in both cell lines was assessed. Skbr3 cells were pre-treated with 3 μ M 6BIO prior to seeding in the upper chamber of the Transwell™ insert. The cells completely migrated in less than 4 hours through the membrane towards the chemoattractant FCS in the lower chamber. L3.6pl cells were seeded in the upper chamber of the insert, stimulated with 3 μ M 6BIO and allowed to migrate towards the FCS in the lower chamber for 20 hours. 6BIO significantly reduced the migration of Skbr3 cells through the 8 μ m pores of the insert (Figure 4.7A) and visibly reduced L3.6pl migration, but not in any significant manner in comparison to the controls (Figure 4.7B).

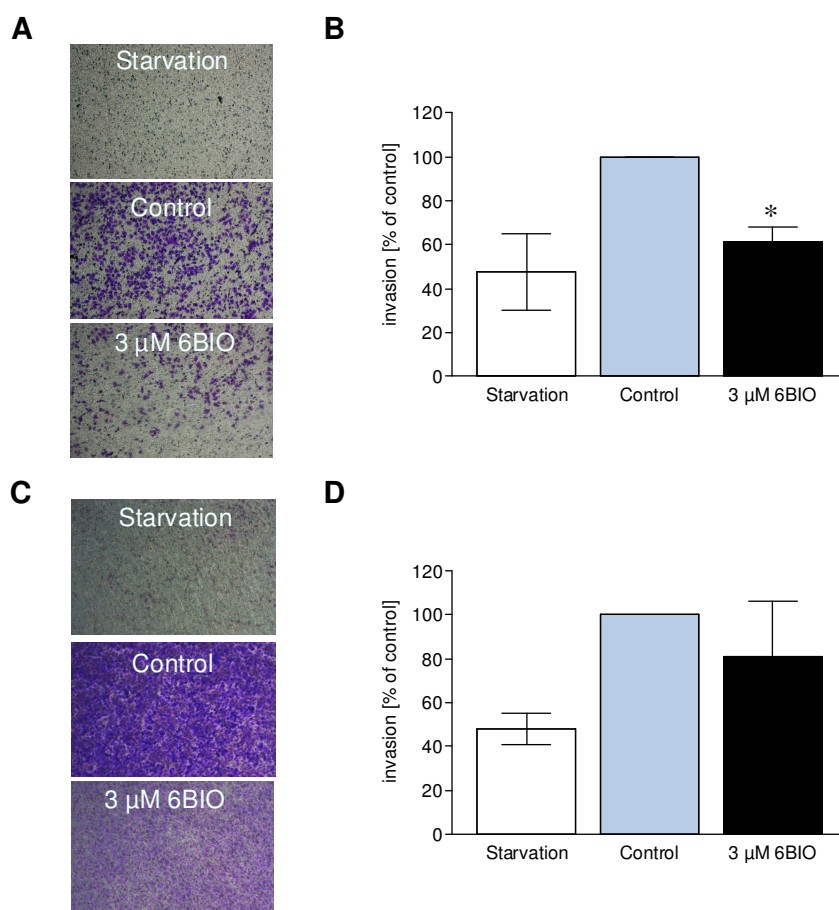


Figure 4.7: Reduction of the tumor cell Transwell™ migration by 6BIO

Skbr3 (A/B) and L3.6pl (C/D) tumor cells were allowed to migrate through 8 μ m pores in a Transwell™ insert towards FCS in the presence or absence of 3 μ M 6BIO treatment. Images on the left (A and C) are representative of migrated cells from triplicate experiments. Graphical analysis on the right (B and D) shows the quantification of migration relative to the control wells. One-way ANOVA/Turkey tests were used to assess significance. Bars are the SEM of three independent experiments performed in duplicate with *, $P < 0.05$.

4.2.3 Effects of 6BIO on Skbr3 chemotaxis in response to a FCS gradient

When presented to a FCS gradient (0-10%), Skbr3 cells will rapidly migrate towards the higher concentration. Skbr3 cells were seeded into an IBIDI™ μ -slide and allowed to adhere before treatment with 6BIO. Thereafter, the cells migrated for a period of 24 hours. The directionality of 50 cells from individual assays were measured and expressed as y-forward values using ImageJ software. The controls were calculated as 1.0, and the y-forward index for the triplicate assays resulted in 1.0 ± 0.264 . The chemotaxis assays treated with $3 \mu\text{M}$ 6BIO showed a y-forward index of 0.367 ± 0.182 . The ImageJ software was used to find the y-center of mass, the Euclidean distance (direct distance between the starting point and end point of a cell track), the accumulated distance, and the velocity at which the cells travel. 6BIO treatment impairs each of these in comparison to the control: y-center of mass (control 1.0 ± 0.194 vs 6BIO 0.317 ± 0.173), Euclidean distance (control 1.0 ± 0.100 vs 6BIO 0.630 ± 0.078), accumulated distance (control 1.0 ± 0.145 vs 6BIO 0.743 ± 0.065). In contrast, velocity was not targeted (control 1.0 ± 0.147 vs 6BIO 0.905 ± 0.189) (Figure 4.8B).

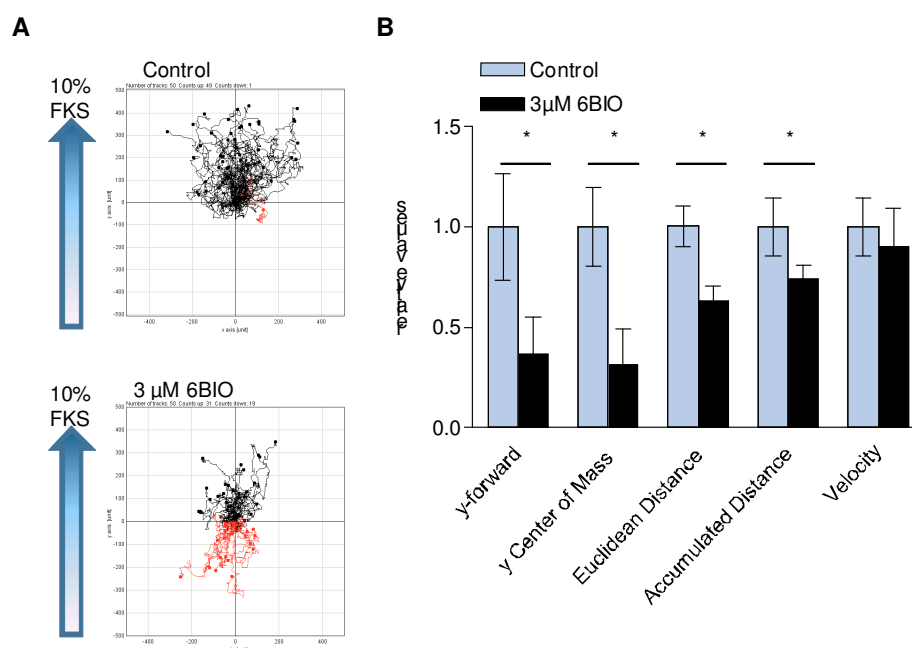


Figure 4.8: Disruption of the directional cell migration by 6BIO

Skbr3 directional migration was impaired in the presence of 6BIO in chemotaxis assays. Skbr3 cells migrated towards a 10% FCS gradient over a 24-hour period. 50 cells from each individual experiment were tracked and analyzed showing that treatment with $3 \mu\text{M}$ 6BIO induced a more random migration pattern (A). Graphical analyses of the parameters were calculated relative to the control set at a relative value of 1. One-way ANOVA/Students t-tests were used to assess significance. Bars are the SEM of three independent experiments with *, $P < 0.05$.

4.2.4 Effects of 6BIO on Skbr3 invasion through Matrigel™

Untreated Skbr3 cells invade through Matrigel™ in response to FCS and fibronectin used as chemoattractants. Skbr3 cells were seeded into the upper well of a Transwell™ insert in the presence of 3 μ M 6BIO and allowed to invade in response to chemoattractants for a period of 20 hours (Figure 4.9A). 3 μ M 6BIO significantly disrupted the invasion of Skbr3 cells (59% relative invaded cells), nearly to that of the controls lacking any chemoattractants (55%) (Figure 4.9B).

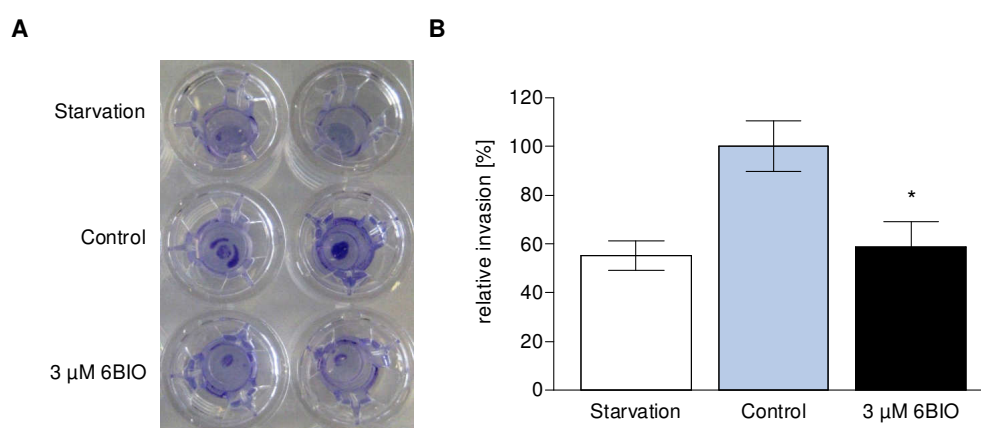
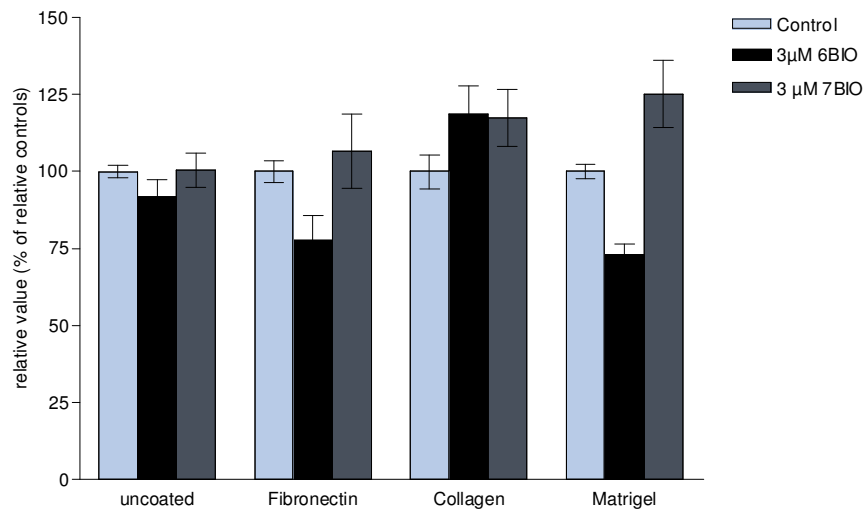
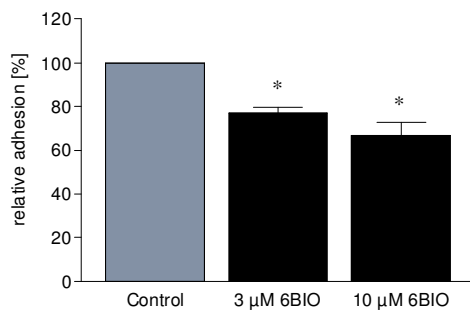


Figure 4.9: Disruption of the Skbr3 invasion through Matrigel™ by 6BIO

Skbr3 cells were seeded into the upper well of a Transwell™ insert and allowed to invade through a layer of Matrigel™ towards the lower chamber containing FCS and fibronectin (Control and 6BIO treated) or no attractants (Starvation). Representative images of invaded cells are shown (A). The graph displays relative invasion of Skbr3 cells with the control cells set to 100% (B). One-way ANOVA/Turkey tests were used to assess significance. Bars are the SEM of three independent experiments performed in duplicate with *, $P < 0.05$.

4.2.5 Effect of 6BIO on tumor cell adhesion

Cellular adhesion is a crucial step in tumor cell metastasis and this process can be up-regulated in circulating tumor cells. To test if 6BIO has any ability to block the adhesion of tumor cells, Skbr3 and L3.6pl cells were allowed to individually adhere for up to 1.5 hours to wells coated with various attractants (fibronectin, collagen G or Matrigel™). Treatment with 6BIO did not significantly reduce the adhesion of L3.6pl to any of the coatings presented (Figure 4.10 A). Skbr3 cells were then tested with two different concentration of 6BIO against 5 μ g/cm² fibronectin coating. Treatment with 6BIO significantly reduced the ability of Skbr3 cells ability to bind to fibronectin by 23% (3 μ M 6BIO) and 33% (10 μ M 6BIO) respective to the controls (Figure 4.10 B).

A L3.6pl**B Skbr3****Figure 4.10: Adhesion of tumor cells to attractants**

L3.6pl cells were seeded and allowed to adhere onto a variety of coated wells and simultaneously treated with 3 μM 6BIO or 7BIO. Neither 6BIO nor 7BIO significantly prevented L3.6pl from binding to any of the coatings with respect to the controls (A).

Skbr3 cells were similarly seeded onto fibronectin-coated wells and stimulated with respective doses of 6BIO, clearly indicating a significant reduction of binding upon 6BIO treatment (B).

One-way ANOVA/Turkey tests were used to assess significance. Bars are the SEM of three independent experiments performed in triplicate with *, $P < 0.05$.

Taken together, treatment with 6BIO, but not with 7BIO, at sub-apoptotic doses significantly reduced adhesion, wound healing capacity, directed migration and invasive capabilities of tumor cells.

4.3 β 1 Integrin expression

β 1 Integrin is essential for adhesion and cell spreading thus playing a key role in migration signaling in tumor cells. α 5 β 1 Integrin is reported to be necessary for binding to fibronectin.⁹⁰⁻⁹¹ Since 6BIO significantly affected the binding of Skbr3 cells to fibronectin (Figure 4.10), expression of β 1 integrin was assessed.

4.3.1 β 1 Integrin expression on the Skbr3 cell surface

Total β 1 integrin surface expression was measured using specific primary anti- β 1 integrin antibodies (Santa Cruz) and secondary Alexa Fluor 488 goat-anti-mouse antibodies (Molecular Signaling/Invitrogen). Antibody-tagged cells were placed into the FACS machine and total mean fluorescence for each sample was measured. Two separate assays were performed applying fibronectin to determine if β 1 integrin surface expression is disrupted.

Initially, Skbr3 cells were allowed to adhere to fibronectin-coated plates as found in the adhesion assay (Figure 4.10) and assessed for β 1 integrin surface expression (Figure 4.11 A and B).

Next, Skbr3 cells were seeded and allowed to migrate over fibronectin for a period of 24 hours with or without 6BIO treatment and the total β 1 integrin surface expression was assessed (Figure 4.11 C and D).

In both experiments, no significant change of surface β 1 integrin expression could be seen in comparison to control samples.

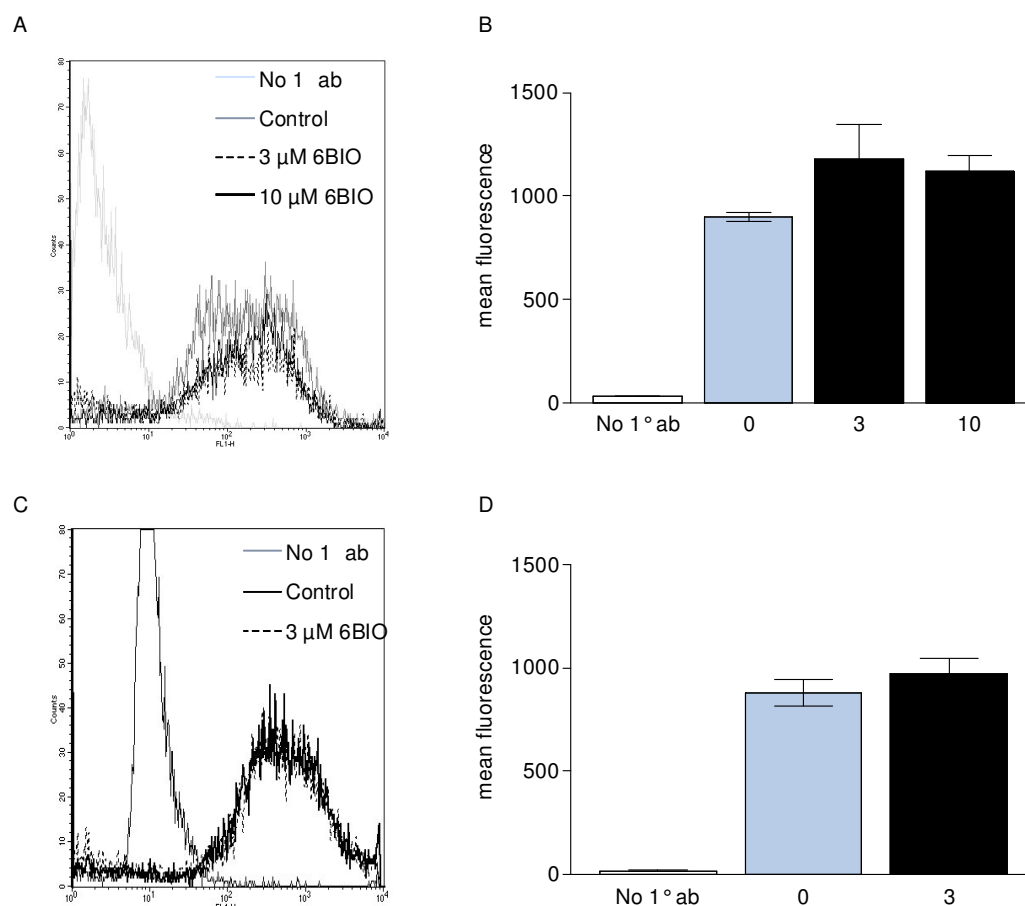


Figure 4.11: Surface $\beta 1$ integrin expression by 6BIO treatment

Total $\beta 1$ integrin expression was measured using specific antibodies toward $\beta 1$ integrin applying FCM analysis of mean fluorescence for each sample. Skbr3 cells were allowed to adhere for 1 hour to fibronectin with or without 6BIO treatment as seen in the histograms (A) or graph (B). Skbr3 cells were allowed to migrate on fibronectin with or without 24-hours of 6BIO treatment as seen in the histograms (C) or in the graph (D).

One-way ANOVA/Turkey tests were used to assess significance. Bars are the SEM of three independent experiments performed in triplicate.

4.3.2 Total $\beta 1$ integrin expression of Skbr3 cells

The $\beta 1$ integrin cycles within the cell as a necessary part of the focal adhesion turnover in the migratory process. Although they lack any known enzymatic activity of their own, integrins can initiate 'outside-in signaling' by recruiting signaling moieties to convey signals to the migratory machinery of the cell.⁶⁵

Although the external expression of $\beta 1$ integrin remained the same (see 4.3.1), this does not account for the entire cycling process of $\beta 1$ integrin. Therefore, expression of the activated and total form were assessed upon Skbr3 adhesion to fibronectin

with or without 6BIO treatment, applying Western blot and CSLM technology. Both assays utilized antibodies specific for the phosphorylation site S785 on $\alpha 5\beta 1$ integrin as well as the total form of $\beta 1$ integrin.

The expression of the total $\beta 1$ integrin increased only slightly, whereas the phosphorylated form increased significantly in comparison to the controls (Figure 4.12). Similar expression levels were seen using CSLM where total $\beta 1$ integrin expression remained similar to that of control wells, but levels of p $\beta 1$ integrin S785 were increased (Figure 4.13).

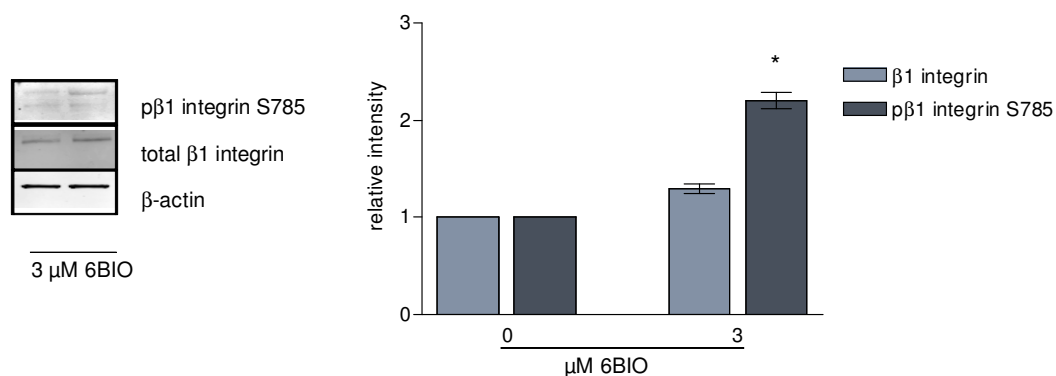


Figure 4.12: Expression of total $\beta 1$ integrin by 6BIO treatment

Skbr3 cells were seeded onto fibronectin coated wells and were allowed to adhere in the presence or absence (Control) of 6BIO for 1 hour. Western blot analysis of lysates from these samples were probed with antibodies against total $\beta 1$ integrin and pS785 $\beta 1$ integrin. Membranes representative from at least two independent experiments are depicted (left) and total protein relative to the controls were analyzed with the ImageJ gel analyzer plugin and represented graphically (right). One-way ANOVA/Turkey tests were used to assess significance. Bars are the SEM of three independent experiments performed in triplicate. * $P < 0.01$.

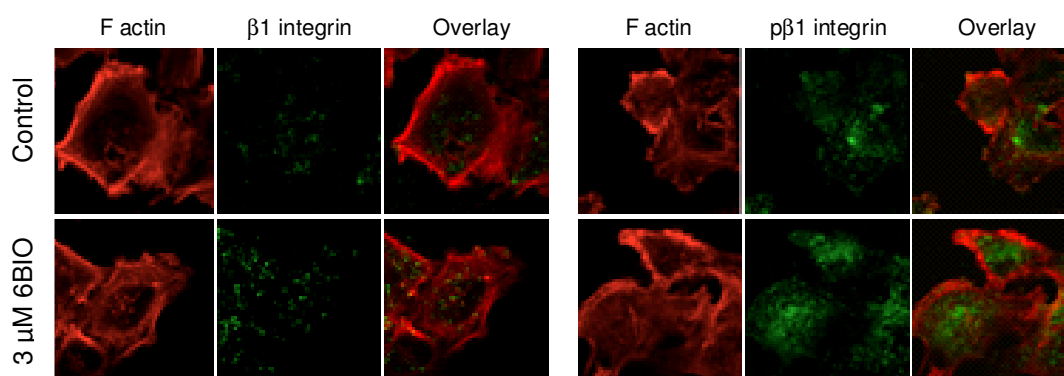


Figure 4.13: Total and active $\beta 1$ integrin expression after 6BIO treatment

Skbr3 cells were seeded onto fibronectin-coated 8-well chamber slides and probed for total $\beta 1$ integrin expression (left) as well as for phospho $\beta 1$ integrin S785 expression (right) with or without 6BIO treatment. Images are representative of at least two independent experiments.

4.4 Effects of 6BIO on migratory signaling pathways

4.4.1 Alteration of Akt expression following 6BIO treatment

Active Akt has been repeatedly shown to be necessary for the formation of focal adhesions in many tumor cells lines.^{64, 81} Akt is translocated to the plasma membrane upon PtdIns-3,4,5-P₃ interaction, where it is then phosphorylated at two sites, first at T308 by PDK1 and then at S473 by PDK2.

Based on the recent inverse kinase screening assay performed with 6BIO and 7BIO, which indicated that PDK1 is a specific kinase target of 6BIO, but not of 7BIO, both phosphorylation sites of Akt and the total form of Akt were probed with antibodies to determine if 6BIO or 7BIO had any effect (Figure 4.14).

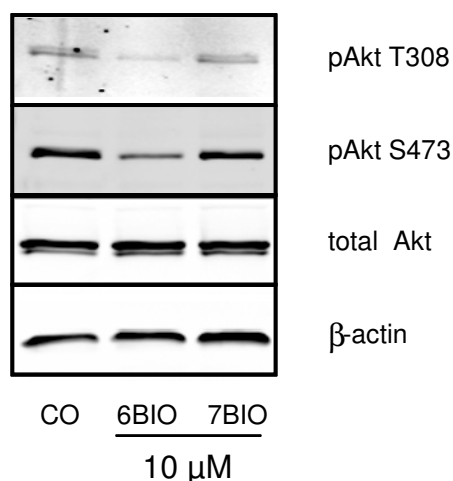


Figure 4.14: Reduction of the activated form of Akt by 6BIO treatment

Skbr3 cells were left untreated (CO) or treated with 10 μM 6BIO or 7BIO for 30 minutes. Active Akt expression was analyzed by Western blot. Equal protein loading was controlled by β-actin. Representative membranes are shown from triplicate experiments.

CSLM was utilized to determine the location of the activated forms Akt using the pT308 antibody for the initial activation (Figure 4.15), and the pS473 antibody for the full activation (Figure 4.16).

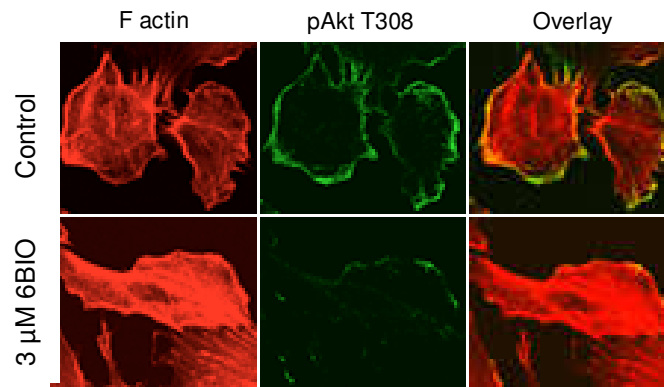


Figure 4.15: Reduction of active Akt localization to lamellipodia by 6BIO treatment

Skbr3 cells were allowed to adhere to 8-well chamber slides prior to stimulation with 3 μM 6BIO for 24 hours. Anti-pT308 Akt antibodies were used to tag active Akt which localizes to the lamellipodia. Images are representative of three independent experiments.

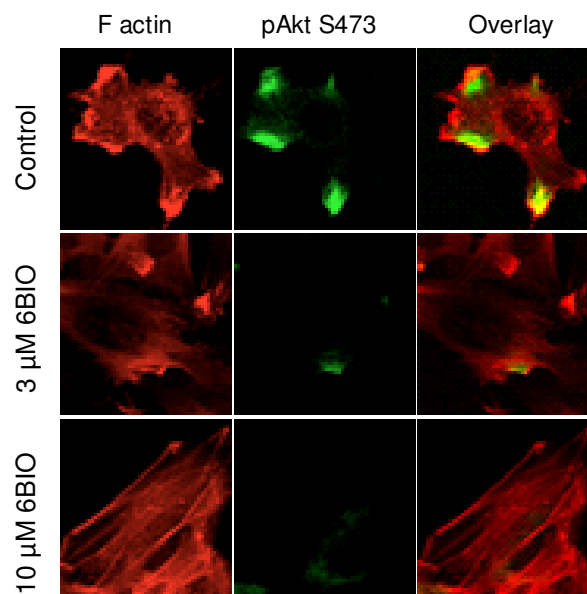


Figure 4.16: Reduction of pS473 Akt cycling by 6BIO treatment

Skbr3 cells were treated with increasing doses of 6BIO or left untreated (Control) for 24 hours. Treatment by 6BIO significantly reduced the expression and location of pS473 in Skbr3 cells. CSLM images are representative of three independent experiments.

4.4.2 Erk and FAK levels following 6BIO treatment

Erk and FAK play prominent roles in the signaling cascades of the migratory systems in tumor cells. Of the six phosphorylation sites on FAK, T397 is the auto-phosphorylation site required for catalytic activity of FAK.⁹² Once phosphorylated, FAK functions as an adapter protein along with integrins to recruit other adhesion and migratory signaling proteins to their regulators, thereby affecting the assembly and disassembly of FAs. FAK directly influences the activity of the Rho GTPase Rac1 through the phosphorylation of activators. Rac1 then activates the MAPK pathway, which in turn activates Erk. The activation of Erk is necessary for proper actin assembly, protrusive abilities and adhesion complex stability.^{80, 92-94}

Stimulation of Skbr3 cells with 3 μ M 6BIO for 30-60 minutes did not affect the phosphorylation sites of Erk at either pT202 or pY204 (Figure 4.17A). This treatment also did not affect pT397 FAK or total FAK expression in Skbr3 cells (Figure 4.17B).

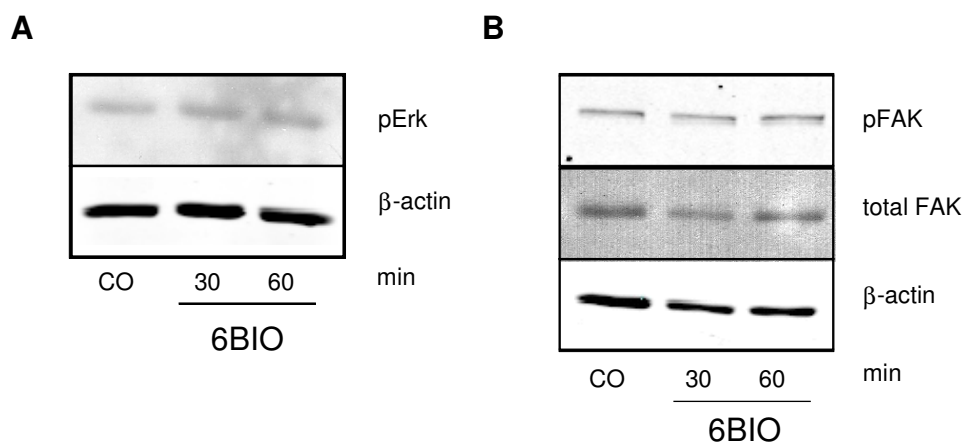


Figure 4.17: Effect on pErk or pFAK/total FAK expression in Skbr3 cells upon 6BIO treatment

Skbr3 cells were seeded and allowed to adhere overnight before stimulation with or without 3 μ M 6BIO for 30 minutes and 1 hour before Western blot analysis for the pT202/Y204 site for Erk, the pT397 FAK and total FAK. The pT202/y204 phosphorylation sites were unaffected by 6BIO treatment (A). pT397FAK and total FAK also showed no significant changes from the control. Protein loading was controlled with β -actin. Images represent at least three independent experiments.

Total FAK in Skbr3 cells was imaged with CSLM after treatment with 6BIO for 24 hours (Figure 4.18). In the CSLM images the total FAK expression within cells was not altered in 6BIO treated cells. However, the distribution of total FAK within the cell was disrupted. Furthermore, the cell morphology was disturbed showing fewer lamellipodia and FAK was significantly hindered from reaching focal adhesions upon 6BIO treatment.

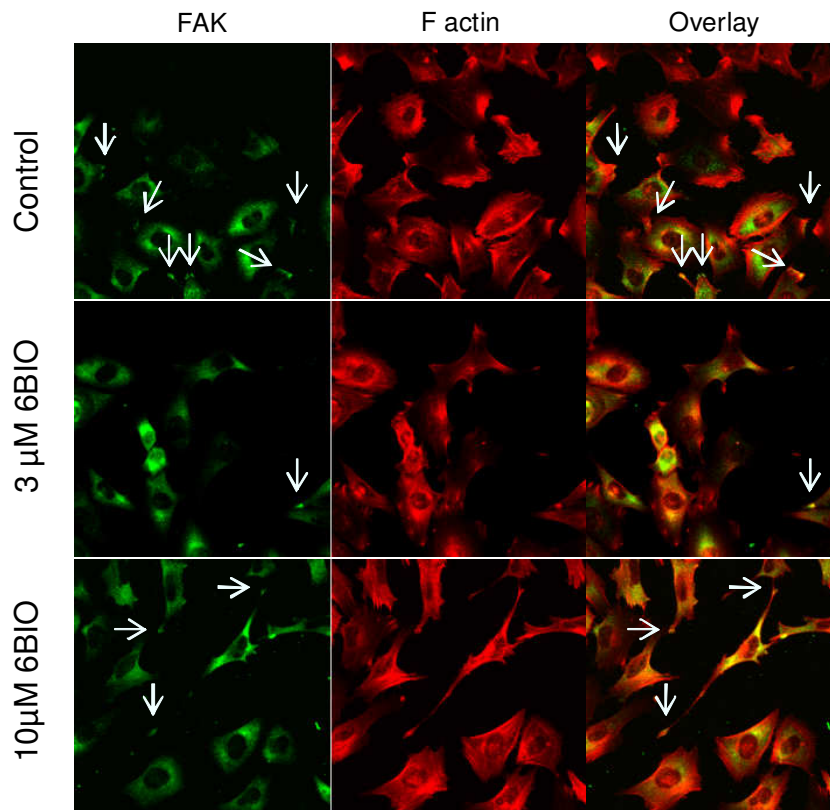


Figure 4.18: Effect of 6BIO treatment on FAK expression and distribution

Skbr3 cells were allowed to adhere prior to a 24-hour stimulation with or without increasing doses of 6BIO. Cells were probed with a total FAK antibody and F actin was stained with rhodamine phalloidin before imaging with CSLM. White arrows indicate FAK expression either at focal adhesions or at lamellipodia. Images are representative of at least two independent experiments.

4.5 Actin cytoskeleton signaling upon 6BIO treatment

The constant cycling and remodeling of actin is necessary throughout the entire cellular migration process and is absolutely essential for the formation of filopodia, lamellipodia and stress fibers.^{59, 95} As demonstrated above, 6BIO has been shown to disrupt adhesion, migration and invasion of Skbr3 cells, all of which may depend on signaling cascades that are linked to actin.

To look now directly at the action of 6BIO against the actin cytoskeleton, migrating Skbr3 cells were fixed, stained for F actin with rhodamine phalloidin as well as probed over various time points with antibodies specific to Rho GTPase Rac1.

4.5.1 Effects on the actin cytoskeleton by 6BIO treatment

Initially, Skbr3 cells were grown in chamber slides and allowed to migrate over a 24-hour time period in the presence of various concentrations of 6BIO. The actin cytoskeletons were stained with rhodamine phalloidin and changes in cellular morphology were noted after extended exposure to 6BIO. Control Skbr3 cells maintained a typical migrating cell morphology: Lamellipodia and filopodia could be found on the leading edge of migrating cells and cellular retraction occurred in the rear end of the cells. Skbr3 cells treated with 3 μM 6BIO showed distortions in the morphology: Fewer lamellipodia were visible and filopodia were longer and appeared to have difficulty in retracting. Treatment with 10 μM 6BIO showed even stronger effects: lamellipodia were nearly completely abolished and the cell took on a more spindle like appearance due to the number of filopodial extensions present (Figure 4.19).

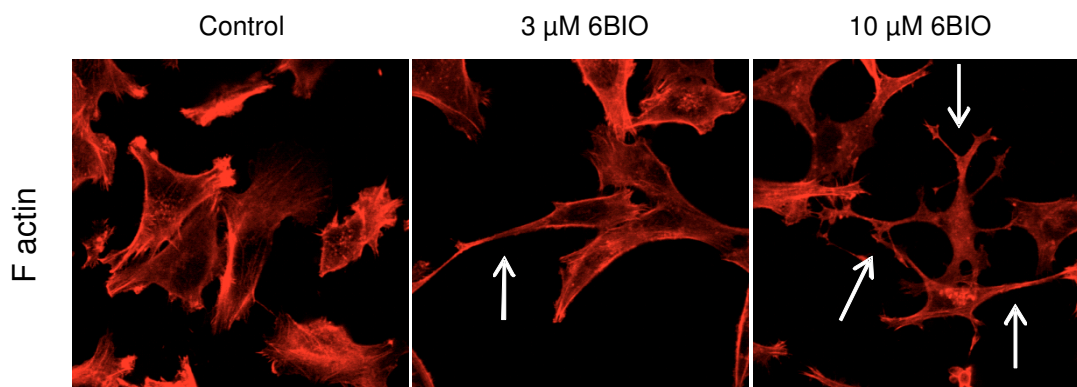


Figure 4.19: Alteration of the actin cytoskeleton in Skbr3 cells upon 6BIO treatment

Skbr3 cells were allowed to migrate for 24 hours in 8-well chamber glass slides with or without increasing 6BIO treatment before fixing and F actin staining with rhodamine phalloidin. Cells were imaged with CLSM and the morphology of the fixed cells was assessed. 6BIO treatment caused large cellular protrusions (white arrows), a significant reduction in lamellipodia, and the cells took on a more spindle like morphology. Representative images shown above represent migrating Skbr3 cells from triplicate experiments stained with rhodamine phalloidin for F actin.

4.5.2 Expression of Rac1 upon 6BIO treatment

Based on the extreme distortion of the actin cytoskeleton in Figure 4.19, the small Rho GTPase Rac1 was investigated because it plays an essential role as a regulator of the actin cytoskeleton in migratory signaling.⁹³ In detail, Rac1 is known to be a crucial regulator during lamellipodia and focal adhesion formation, as well to provide an essential signal required for the forward migration of moving cells.⁶⁴

The expression of the active form of this GTPase was investigated using a pull-down assay (Figure 4.20).

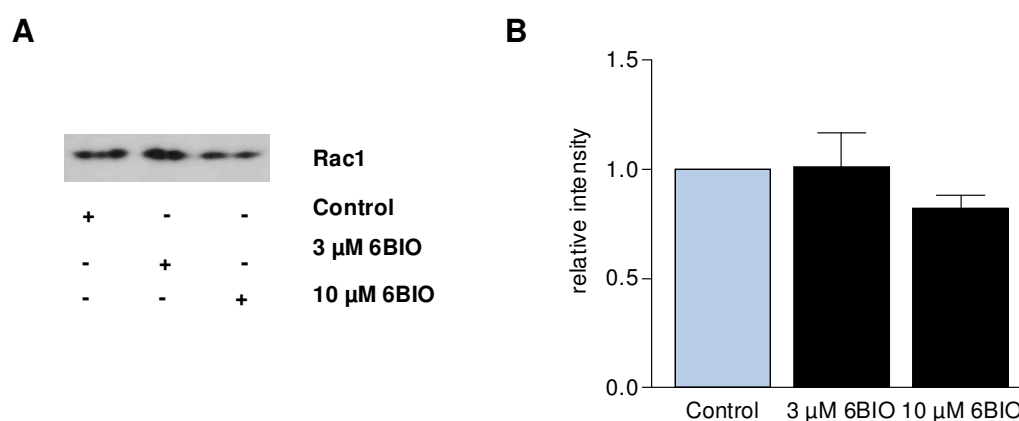


Figure 4.20: Effect of 6BIO treatment on active and total Rac1 expression

The active form of Rac1 was measured using a pull-down assay and Western blotting as described in Materials and Methods (A). The gel analyzer plugin for ImageJ was utilized to quantify the amount of active Rac1 (B). One-way ANOVA/Turkey tests were used to assess significance. Bars are the SEM of at least three independent experiments.

Treatment by 6BIO visibly, but not significantly affected the active expression Rac1 in Skbr3 cells. These findings were verified by CSLM staining (Figure 4.21). Since the lamellipodia were so clearly affected by 6BIO treatment as seen in Figure 4.19, Skbr3 cells were grown in 8-well fibronectin-coated slides for CSLM analysis and probed for Rac1 expression. It is known that the migratory signaling molecules must be constantly refreshed through their recycling through the cell. Skbr3 cells were probed for Rac1 to determine if this cycle is somehow disrupted by 6BIO treatment. Rac1 levels appeared similarly expressed in Skbr3 cells with or without 6BIO treatment. The amount of lamellipodia was reduced in 6BIO-treated cells, and the recycling of Rac1 is visibly disrupted as seen in Figure 4.21.

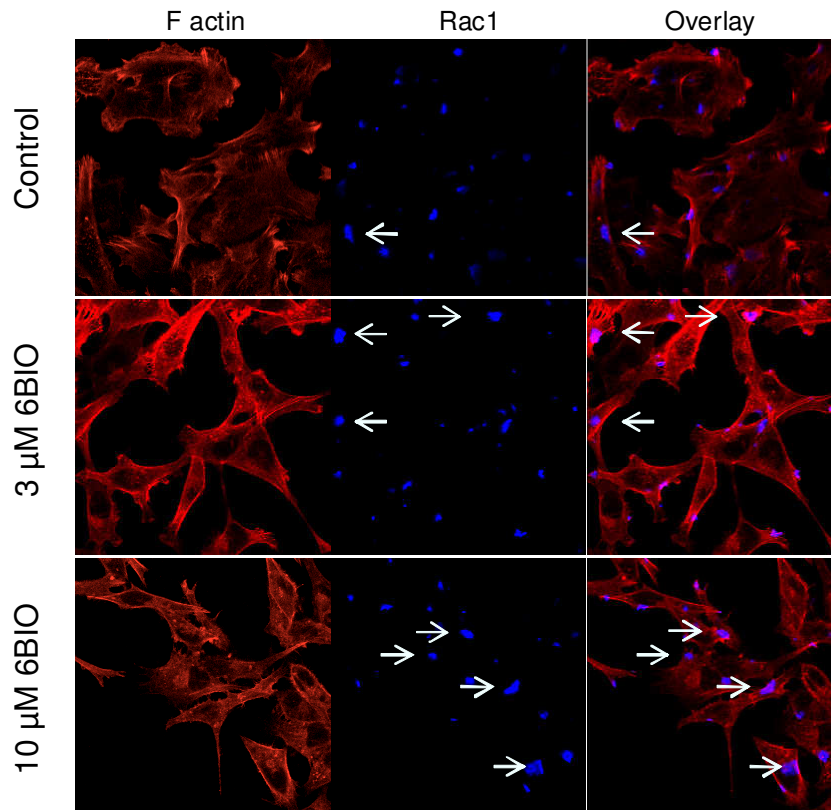


Figure 4.21: Effect of 6BIO on Rac1

Skbr3 cells were seeded thinly and allowed to adhere to fibronectin-coated 8-well chamber slides before 24 hours of treatment with 6BIO. Cells were fixed and probed with Rac1 antibodies and imaged with CSLM. Treatment with 6BIO reduces lamellipodia formation and white arrows indicate Rac1 located at the center of the cell, rather than at focal adhesion or the leading edge. Images are representative of three independent experiments performed in duplicate.

4.6 Effects of 6BIO on 3D spheroids

Skbr3 cells are quite amenable to spheroid formation, and it is well supported that 3D spheroid potentially recreate the tumor microenvironment.⁸⁹

4.6.1 Disruption of Skbr3 and fibroblast spheroids 6BIO treatment

For the evaluation of the 6BIO treatment on the spheroid structure, Skbr3 spheroids and fibroblast spheroids as well were cultivated. Spheroids were individually treated with a range of concentrations of 6BIO for up to 165 hours. 6BIO significantly disrupted the spheroids already at a 5 μM concentration (Figure 4.22).

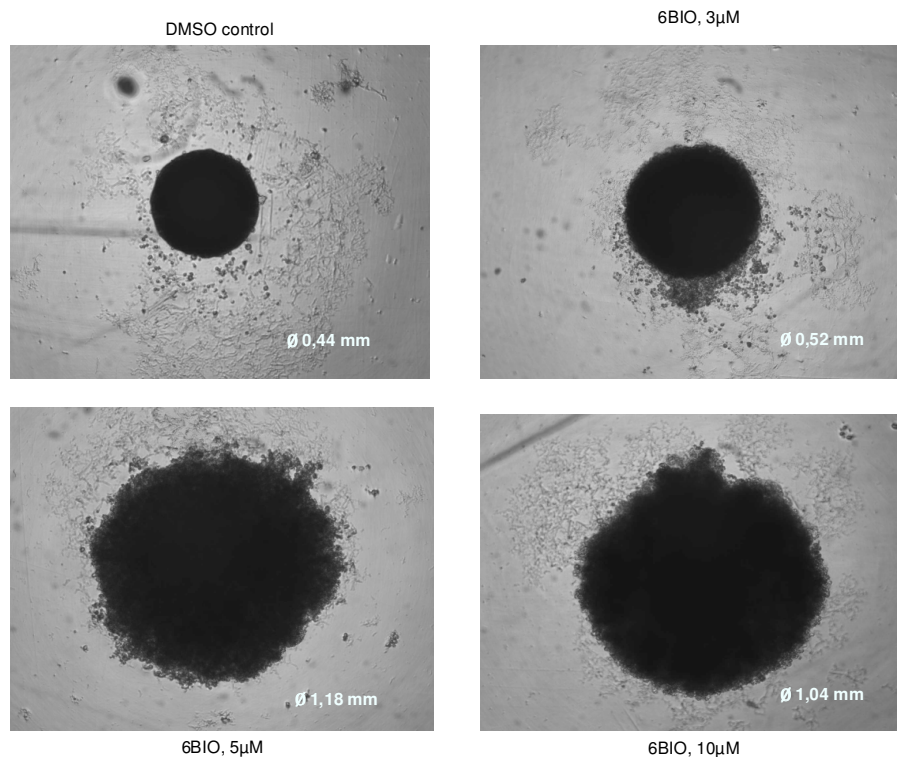


Figure 4.22: Images of Skbr3 spheroids treated with 6BIO

Skbr3 spheroids were cultivated and treated for 165 hours with or without increasing doses of 6BIO. Spheroids were disrupted in a dose-dependent manner beginning with 5 μM of 6BIO. Images are representative of multiple images taken.

Furthermore, MTT was added to the individual spheroids to measure their metabolic activities. Both spheroid types showed reduced metabolic activities in a dose-dependent manner (Figure 4.23).

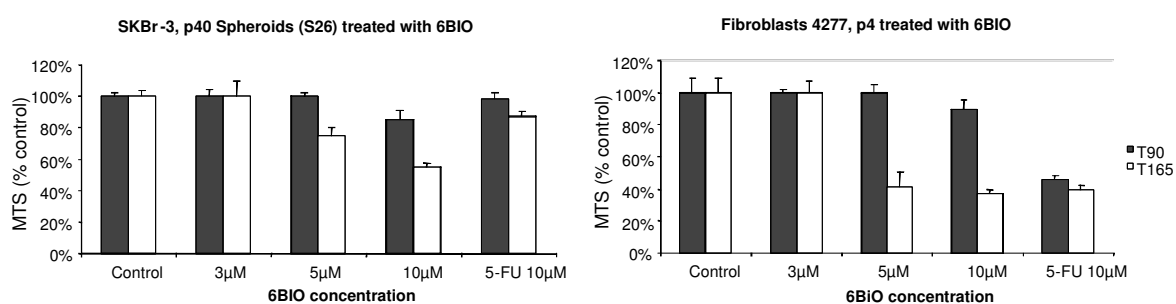


Figure 4.23: Reduction of the metabolism of Skbr3 and fibroblast spheroids by 6BIO

MTT was added to the Skbr3 spheroids (left) as well as to fibroblast spheroids (right) treated with increasing doses of 6BIO. The graphical analysis shows the results at 90 hours (T90 black) and 165 hours (T165 white) of treatment with 6BIO in comparison to the well-known chemotherapeutic drug 5-fluorouracil (5-FU). The effects of 6BIO on spheroid metabolism are dose-dependent.

4.6.2 Disruption of Skbr3 spheroid invasion by 6BIO

in a confrontation assay

Skbr3 spheroids were challenged with fibroblast spheroids in a spheroid confrontation assay as described in Materials and Methods. Stimulation with 6BIO visibly reduced the migratory and invasive capabilities of Skbr3 spheroids to invade the fibroblast spheroids. All tested doses of 6BIO effectively reduced the migration, as can be seen in Figure 4.24.

When confronted, the Skbr3 cells clearly invade both themselves and the fibroblast spheroids, whereas the fibroblast spheroids remain separate throughout the entire experiment.

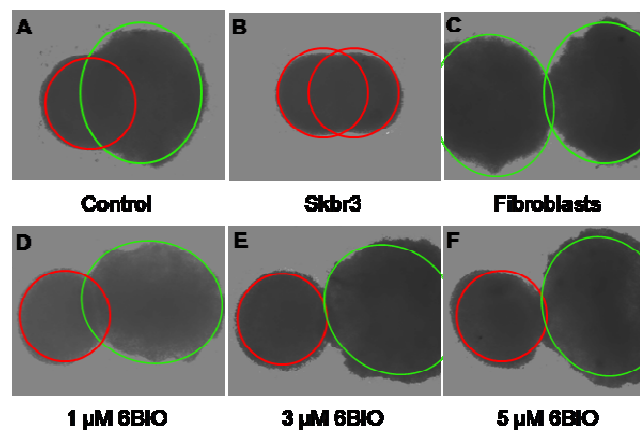


Figure 4.24: Reduction of migration and invasion of Skbr3 spheroids by 6BIO

Skbr3 spheroids (circled in red) and fibroblast 4277 P8 spheroids (circled in green) were confronted in individual wells in a 96-well plate. Skbr3 spheroids migrate and invade into fibroblast 4277 P8 spheroids (A) and into themselves (B), whereas the fibroblast 4277 P8 spheroids remain separate when confronted with another fibroblast (C). Treatment with 6BIO blocks this migration in a dose-dependent manner (D-F). The images shown are representative of a series of confrontations.

5 DISCUSSION

The main cause of cancer death is not due to the primary tumor itself, but to the metastasis thereof. By targeting these deregulated pathways with new chemotherapeutic drugs more effective treatment of the primary tumor can be realized, thereby allowing for a higher cancer eradication rate and potentially a better quality of life.

In our study, two indirubin derivatives, namely 6BIO and 7BIO, show strong potential as anticancer agents, with 6BIO exhibiting highly specific antimetastatic activity through its interaction with PDK1 and the resulting regulation of Akt.

5.1 Virtual comparison of 6BIO and 7BIO

In recent years, protein kinases have proven themselves to be attractive targets for cancer therapeutics.^{1, 96} Although they are a promising category of anticancer drugs, kinase inhibitors are associated with many side effects due to their broad promiscuity of targets. This issue led to the inverse screening approach of several indirubin derivatives to predict their main target(s).¹¹ 6BIO and 7BIO are nearly identical derivatives of indirubin-3'-oxime, differing only in the location of the single bromine halogenation on the 6' and 7' carbon of the istatin ring respectively.³¹ This minute variation allows for astounding differences in their respective targets to elicit their antitumor activities.

In the inverse kinase screening assay,¹¹ it was revealed that 6BIO, but not 7BIO, was highly selective for the PDK1 kinase among other targets. Computer generated modeling studies clearly showed that PDK1 and 6BIO displayed perfect interaction geometries with the binding-pocket of PDK1 being easily able to accommodate the bromine atom. Contrary to this, 7BIO had poor interaction geometries with PDK1. To support these virtual predictions, a preliminary *in vitro* kinase assay specific for PDK1 showed that the IC₅₀ value of 6BIO is 1.5 μ M in comparison to 7BIO which ranked at > 100 μ M.¹¹

5.2 Antitumor activities of 6BIO and 7BIO

To investigate the antitumor activities of the indirubin derivatives, two highly varied cell lines were selected: the breast cancer cell line Skbr3 and the pancreatic cell line L3.6pl. The indirubin derivatives induced apoptosis in both cell lines in a time- and dose-dependent manner, with Skbr3 cells requiring a longer time period for the effects to be fully seen. When the cell lines were forced to remain in an anti-adhesive state which mimics circulation throughout the body, both 6BIO and 7BIO showed anoikis-inducing effects. In addition, both 6BIO and 7BIO had very strong anti-proliferative properties, also occurring in a dose- and time-dependent manner.

Thus, our data strongly confirmed the antitumor activities of 6BIO and 7BIO as predicted by results of Zahler et al.¹¹

5.3 Migration, invasion and adhesion are all disrupted after exposure to 6BIO or 7BIO

Breast cancer is one of the leading causes of cancer death worldwide in women, but approximately only 6% of newly diagnosed patients will have either advanced or metastatic breast cancer. These statistics elevate to nearly 40% of patients who are initially diagnosed with the disease which will eventually progress to the metastatic form.⁹⁷ Cancer metastasis comprises of a complex cascade of events, many of which require integrins, FAK, PDK1/Akt and actin to successfully execute signaling pathways in migration, adhesion and invasion.^{51, 80, 98} Therefore, single drug-based therapeutic interventions to avoid or to reduce metastasis are often quite inefficient.

The inverse kinase screening assay indicated that 6BIO was highly selective for PDK1 and our *in vitro* assays support both 6BIO and 7BIO as antitumor agents.¹¹ PDK1 is ubiquitously expressed in mammalian tissues and plays a key role in the Akt signaling.⁷⁰ Akt, which is activated upon PI3K activation, plays a crucial role in cell signaling pathways downstream of activated receptors located in focal contacts. Mounting evidence indicates that the PI3K-Akt signaling pathway promotes cell motility in tumor cells through its regulation of many signaling pathways and its link to the actin cytoskeleton.⁶⁴

At sub-apoptotic doses 6BIO, but not 7BIO, significantly reduced the migration of both cell lines, nearly halting them completely in wound healing assays *in vitro*. Additionally, both the Skbr3 and the L3.6pl cells lost their ability to invade through membranes in response to chemoattractants. Chemotaxis of Skbr3 cells towards a gradient of FCS was dramatically disrupted upon 3 μ M 6BIO treatment. The Skbr3 cells showed significant disruption of their γ -forward movement towards the chemoattractant gradient, indicating that cells were no longer able to polarize properly. The Euclidean distance and the total distance traveled by the Skbr3 cells were also significantly altered, indicating that the invasive signaling pathways were no longer functioning properly. Moreover, Skbr3 cells were highly impaired in their ability to invade through MatrigelTM layers in response to multiple chemoattractants. Finally, the adhesion of Skbr3 tumor cells to fibronectin was reduced through 6BIO stimulation. Taken together, these results indicate that 6BIO has very strong anti-metastatic properties, which were not shown so far in the literature.

5.4 β 1 Integrin and the actin cytoskeleton

Integrin-mediated migration is a complex process regulated by signaling cascades which control the actin cytoskeleton in response to microenvironmental signals to polarize the cell, extend the cellular membrane through protrusion and adhesion formations, translocate the cell body, and finally disassemble adhesions and rear retraction.⁷⁹ Integrins are transmembrane receptors, mechanical links between extracellular signals, and the interior structural and signaling molecules which control the actin cytoskeleton.⁷⁸

β 1 Integrin is essential for adhesion, cell spreading, and plays a key role in migration signaling in tumor cells. Although they lack any known enzymatic activity of their own, integrins can initiate 'outside-in' signaling by recruiting signaling moieties (such as FAK) that generate and convey signals to the migratory and proliferative machinery of the cell.⁶⁵ Integrins are trafficked by the endosomal pathway and it is thought that these pathways and the recycling of integrins help to drive cell migration by moving adhesion receptors from the back to the front of moving cells.⁹⁹ α 5 β 1 Integrin is reported to be essential for binding of the cells to fibronectin.⁹⁰⁻⁹¹

As 6BIO significantly affected the binding of Skbr3 cells to fibronectin (Figure 4.10), expression of $\beta 1$ integrin was assessed, however the total form was not altered upon 6BIO treatment. In this context our experiments were unable to support the findings of Liu et al., which suggested $\beta 1$ integrin as a downstream target of PDK1 through Akt.¹⁰

According to the research done by Mulrooney et al.,⁸⁴ a decrease in the pS785 $\beta 1$ integrin promotes cell spreading and directed cell migration, whereas an increase in the pS785 $\beta 1$ integrin enhances attachment but inhibits cell spreading or migration in teratocarcinoma cells. In our experiments, the effects of 6BIO treatment on Skbr3 cells appeared to increase the total amount of pS785 $\beta 1$ integrin, which coincides with the disruption of migration published by Mulrooney et al.⁸⁴

The actin cytoskeleton was clearly disrupted upon 24-hour stimulation with 6BIO. The cells took on a more spindle-like appearance, losing the rounded edges and many of the lamellipodia. They appeared to be unable to retract filopodia and recycle the actin components necessary for migration. The increased amount of pS785 $\beta 1$ integrin and the ability of 6BIO to preferentially bind to PDK1, thereby lacking of full Akt activation are two of the most likely contributors to the disruption of the actin cytoskeleton.

5.5 Metastatic signaling targets

Several major signaling cascades are understood to be the main controlling factors in cellular adhesion and migration, which center around integrins, FAK and targets thereof. The major autophosphorylation site of FAK (Tyr-397) is the binding site for the SH2 domain of p85 and is responsible for the *in vivo* association of FAK with PI3K, which can subsequently activate PI3K during cell adhesion.¹⁰⁰ FAK is also attributed to the recruitment and activation of signaling molecules (Cas-Crk-DOCK-ELMO) which stimulate and localize activation of Rac1 and its effectors. Some of them are thought to be responsible for actin assembly, protrusive activity or modulation of the adhesion complex stability.⁹² Additionally, FAK is also directly linked to Erk through the activation of signaling molecules (Shc or Grb2), which

interact with Ras and Raf to phosphorylate and activate MAP kinase kinases (MEKs) which phosphorylate and activate Erk.⁹⁴ This Raf/MEK/Erk cascade is directly responsible for regulating intra-nuclear transcription factors, thereby inducing cell migration and proliferation.¹⁰¹

Recent reports suggest that PDK1, a well known upstream effector of Akt, plays a major role in breast cancer migration through the regulation of Akt signaling pathways involved in migration, including LIM kinase and cofilin which control actin polymerization.^{10, 69, 102} Through the regulation of $\beta 1$ integrin adhesion as well as cellular migration are affected.^{10, 69, 83} Akt has been shown to be essential in endothelial cells and fibroblasts for the inside-out activation of fibronectin assembly through the activation of $\alpha 5\beta 1$ integrin, which in turn, mediates matrix assembly.⁶⁷

6BIO treatment of the tumor cells did not affect the overall expression levels of Akt, but it did affect both of the phosphorylated forms of Akt. Immunohistochemistry results supported this finding, indicating that 6BIO blocks the activation of pT308 Akt and thereby pS473 of Akt. Together, these observations support the data of the PDK1 kinase assay¹¹ and our migratory data.

Additionally, 6BIO did not strongly affect FAK, Rac1 or Erk. The active forms of these signaling molecules were not significantly altered upon 6BIO treatment. Immunohistochemistry results confirmed these findings, but also indicated that the metastatic signaling cycles were disrupted. FAK was no longer able to return to the cell front, and lamellipodia were unable to properly form. These signaling data suggest for the first time that 6BIO affects the metastatic signaling pathway through the regulation of Akt.

5.6 Effects of 6BIO on Skbr3 and fibroblast spheroids

Spheroid cultures of cancer cells may better reflect characteristics of micro-metastases than traditional monolayer cultures. Therefore, spheroids may be more convenient for cancer drug discovery as they quite accurately model the tumor microenvironment which leads to more relevant physiological out-comes.¹⁰³⁻¹⁰⁴

Furthermore, low-passage cancer cell lines recapitulate the properties of the original tumor cells more closely than commonly used standard cell lines that experience artificial selection processes and mutations over years of passaging.¹⁰⁴

In our experiments, 6BIO reduced the metabolic capabilities of Skbr3 spheroids and fibroblast spheroids already at a 5 μ M dose and caused the dissolution of spheroid structures at higher doses. Moreover, in a confrontation assay, Skbr3 spheroids were blocked from migrating and invading into fibroblast spheroids upon very low doses of 6BIO treatment, suggesting that 6BIO may also be highly effective in metastatic tumor models.

Altogether, this study suggests that both 6BIO and 7BIO are strong antitumor candidates with different modes of action. 6BIO is especially of interest because it could be proven that the substance has significant anti-metastatic properties already at sub-apoptotic doses.

Metastatic cancers are horrific diseases with little to no potential cures. However, our promising cell experimental data supports the further development of 6BIO as an anti-metastatic substance first for application in animal models and finally for clinical use.

6 SUMMARY

The presented work reports the following new findings with the experimental chemotherapeutic indirubin derivatives 6BIO and 7BIO:

6BIO and 7BIO have antitumor properties

Apoptosis induction was investigated in highly invasive breast adeno-carcinoma (Skbr3) and pancreatic tumor (L3.6pl) cell lines. In both cell lines, cell death could be induced proving the usability of 6BIO and 7BIO for cancer treatment. Interestingly, the mechanisms of action of these two substances indicate that they evoke cell death through different modes of action. Thus, these highly selective indirubin derivatives show strong potential as antitumor agents.

6BIO, but not 7BIO, significantly affects metastatic pathways in tumor cells

Astoundingly 6BIO, but not 7BIO, significantly reduced the migration of tumor cells, nearly halting them completely in the Skbr3 wound healing assay at sub-apoptotic doses. Chemotaxis was dramatically disrupted and tumor cells significantly lost their ability to invade through membranes or Matrigel™ layers in response to chemoattractants. Additionally, adhesion of Skbr3 tumor cells to fibronectin was reduced by 6BIO application. Taken together, these results indicate that 6BIO has very strong anti-metastatic properties.

Akt signaling is disrupted by 6BIO, but not by 7BIO

PDK1 is a kinase target of 6BIO, but not of 7BIO, as seen in both the inverse kinase screening assay as well as in the *in vitro* kinase assay.¹¹ By utilizing Western blot technology 6BIO, but not 7BIO, was shown to block the activation of Akt, the downstream target of PDK1. Additionally, CSLM technology clearly showed that the initial phosphorylation site pT308 of Akt is significantly down-regulated, and Akt was no longer able to translocate to the lamellipodia in migrating cells. Moreover, it could be proven that the second phosphorylation site, pS473 of Akt, was

significantly reduced in 6BIO-treated cells in comparison to control cells. Interestingly, treatment of migrating Skbr3 cells by 6BIO indicates that the reduction of dual-phosphorylated Akt severely affects the actin structure and the proper cycling of migratory signaling.

Metastatic signaling and the actin cytoskeleton is affected by 6BIO treatment

Rac1, FAK and Erk are all essential regulators of various components of the actin cytoskeleton in migrating tumor cells.^{59, 63-64, 92, 95, 105} First experiments indicated that 6BIO does not immediately reduce any of these key signaling pathways upon adhesion or during migration of Skbr3 cells. Furthermore, the immunohistochemical results suggested that the metastatic signaling cascades are affected, and these signaling molecules are unable to properly cycle within the cell. The actin cytoskeleton was disrupted by treatment with 6BIO, resulting in a more spindle-like formation and significant reduction in lamellipodia.

β 1 Integrin is affected by 6BIO treatment

β 1 Integrin is essential in the formation of focal contacts and for the proper cycling of metastatic signaling. Treatment of Skbr3 cells with 6BIO disrupts this signaling and increases the amount of pS785 β 1 found in the cells. An increase of pS785 has been linked to decreased motility in teratocarcinoma cells.⁸⁴

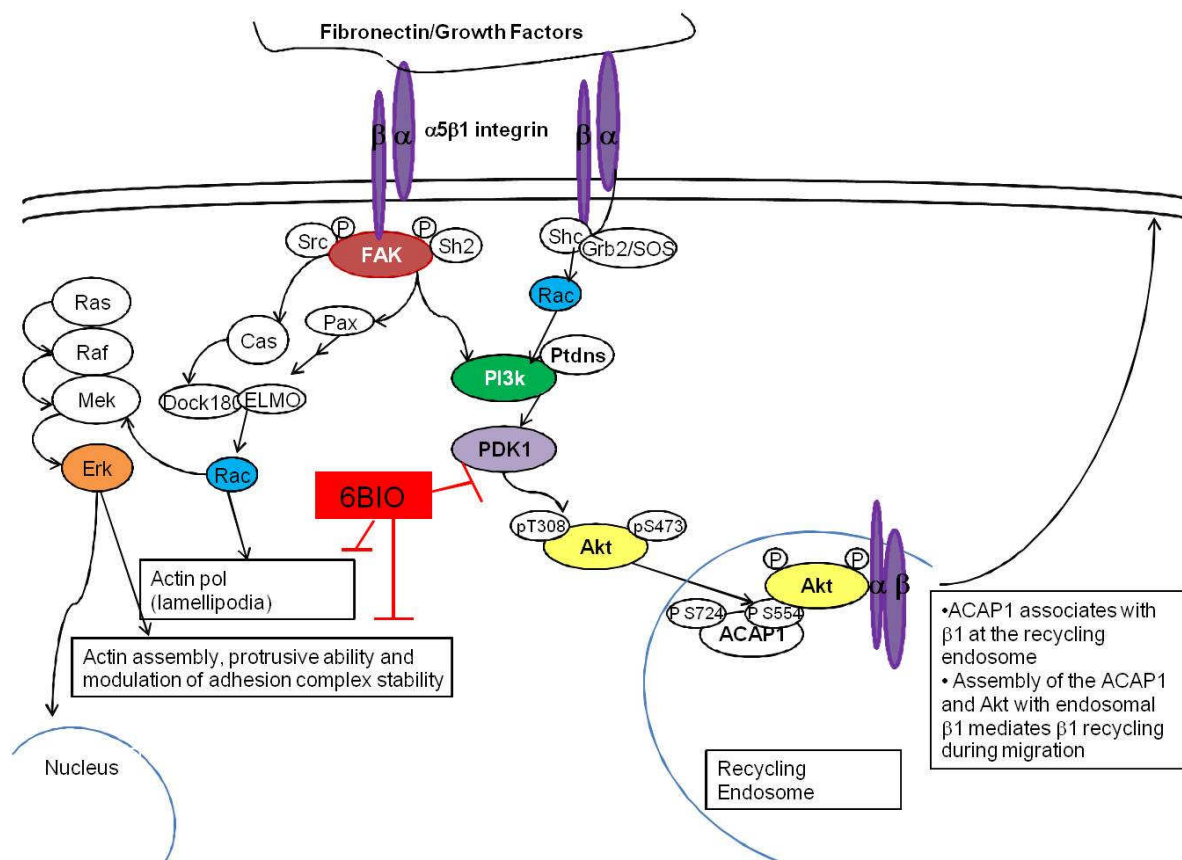
6BIO significantly affects Skbr3 and fibroblast spheroids

Spheroids are considered to be very beneficial to cancer drug discovery as they more accurately model the tumor microenvironment which leads to more relevant physiological outcomes.¹⁰³⁻¹⁰⁴ 6BIO reduced the metabolic capabilities of Skbr3 spheroids and fibroblast spheroids already at low doses and caused the dissolution of spheroid structures at higher doses. Skbr3 spheroids were blocked from migrating and invading into fibroblast spheroids upon very low doses of 6BIO treatment, suggesting that 6BIO might also be highly effective in metastatic tumor models.

Taken together, the experimental indirubin derivatives 6BIO and 7BIO show strong potential as antitumor substances through completely different modes of action.

6BIO especially is of note in that it is capable of inducing apoptosis, not only in arresting tumor cells, but it strongly inhibits tumor cell migration, invasion and adhesion, even at lower concentrations via interfering with a variety of metastatic signaling events as summarized in Figure 6.1

Thereby this substance is suggested as a promising potential therapeutic agent in treatment of metastatic cancer.



7 REFERENCES

1. Hennessy BT, Smith DL, Ram PT, Lu Y, Mills GB. Exploiting the PI3K/AKT pathway for cancer drug discovery. *Nat Rev Drug Discov* 2005;4(12):988-1004.
2. Morales-Ruiz M, Fulton D, Sowa G, Languino LR, Fujio Y, Walsh K, et al. Vascular endothelial growth factor-stimulated actin reorganization and migration of endothelial cells is regulated via the serine/threonine kinase Akt. *Circ Res* 2000;86(8):892-6.
3. Stambolic V, Suzuki A, de la Pompa JL, Brothers GM, Mirtsos C, Sasaki T, et al. Negative regulation of PKB/Akt-dependent cell survival by the tumor suppressor PTEN. *Cell* 1998;95(1):29-39.
4. Alessi DR, James SR, Downes CP, Holmes AB, Gaffney PR, Reese CB, et al. Characterization of a 3-phosphoinositide-dependent protein kinase which phosphorylates and activates protein kinase Balpha. *Curr Biol* 1997;7(4):261-9.
5. Vanhaesebroeck B, Alessi DR. The PI3K-PDK1 connection: more than just a road to PKB. *Biochem J* 2000;346 Pt 3:561-76.
6. Fresno Vara JA, Casado E, de Castro J, Cejas P, Belda-Iniesta C, Gonzalez-Baron M. PI3K/Akt signalling pathway and cancer. *Cancer Treat Rev* 2004;30(2):193-204.
7. Liang K, Lu Y, Li X, Zeng X, Glazer RI, Mills GB, et al. Differential roles of phosphoinositide-dependent protein kinase-1 and akt1 expression and phosphorylation in breast cancer cell resistance to Paclitaxel, Doxorubicin, and gemcitabine. *Mol Pharmacol* 2006;70(3):1045-52.
8. Xie Z, Zeng X, Waldman T, Glazer RI. Transformation of mammary epithelial cells by 3-phosphoinositide- dependent protein kinase-1 activates beta-catenin and c-Myc, and down-regulates caveolin-1. *Cancer Res* 2003;63(17):5370-5.
9. Di Cosimo S, Baselga J. Targeted therapies in breast cancer: where are we now? *Eur J Cancer* 2008;44(18):2781-90.
10. Liu Y, Wang J, Wu M, Wan W, Sun R, Yang D, et al. Down-regulation of 3-phosphoinositide-dependent protein kinase-1 levels inhibits migration and experimental metastasis of human breast cancer cells. *Mol Cancer Res* 2009;7(6):944-54.

11. Zahler S, Tietze S, Totzke F, Kubbutat M, Meijer L, Vollmar AM, et al. Inverse in silico screening for identification of kinase inhibitor targets. *Chem Biol* 2007;14(11):1207-14.
12. Harvey AL. Natural products in drug discovery. *Drug Discov Today* 2008;13(19-20):894-901.
13. Butler MS, Newman DJ. Mother Nature's gifts to diseases of man: the impact of natural products on anti-infective, anticholesteremics and anticancer drug discovery. *Prog Drug Res* 2008;65:1, 3-44.
14. Cragg GM, Grothaus PG, Newman DJ. Impact of natural products on developing new anti-cancer agents. *Chem Rev* 2009;109(7):3012-43.
15. Newman DJ. Natural products as leads to potential drugs: an old process or the new hope for drug discovery? *J Med Chem* 2008;51(9):2589-99.
16. Li JW, Vederas JC. Drug discovery and natural products: end of an era or an endless frontier? *Science* 2009;325(5937):161-5.
17. Borchardt JK. The Beginnings of Drug Therapy: Ancient Mesopotamian Medicine. *Drug News Perspect* 2002;15(3):187-92.
18. Graham JG, Quinn ML, Fabricant DS, Farnsworth NR. Plants used against cancer - an extension of the work of Jonathan Hartwell. *J Ethnopharmacol* 2000;73(3):347-77.
19. Farnsworth NR, Akerele O, Bingel AS, Soejarto DD, Guo Z. Medicinal plants in therapy. *Bull World Health Organ* 1985;63(6):965-81.
20. Fabricant DS, Farnsworth NR. The value of plants used in traditional medicine for drug discovery. *Environ Health Perspect* 2001;109 Suppl 1:69-75.
21. Rishton GM. Natural products as a robust source of new drugs and drug leads: past successes and present day issues. *Am J Cardiol* 2008;101(10A):43D-49D.
22. Mann J. Natural products in cancer chemotherapy: past, present and future. *Nat Rev Cancer* 2002;2(2):143-8.
23. Morgan DO. Principles of CDK regulation. *Nature* 1995;374(6518):131-4.
24. Balfour-Paul J. *Indigo*. London: British Museum Press; 1998.
25. Meijer L SJ, Bettayeb K, Ferandin Y. Diversity of the intracellular mechanisms underlying the anti-tumor properties of indirubins. *International Congress Series* 2007;1304:60-74.

26. Adachi J, Mori Y, Matsui S, Takigami H, Fujino J, Kitagawa H, et al. Indirubin and indigo are potent aryl hydrocarbon receptor ligands present in human urine. *J Biol Chem* 2001;276(34):31475-8.
27. Blanz J, Ehninger G, Zeller KP. The isolation and identification of indigo and indirubin from urine of a patient with leukemia. *Res Commun Chem Pathol Pharmacol* 1989;64(1):145-56.
28. Eisenbrand G, Hippe F, Jakobs S, Muehlbeyer S. Molecular mechanisms of indirubin and its derivatives: novel anticancer molecules with their origin in traditional Chinese phytomedicine. *J Cancer Res Clin Oncol* 2004;130(11):627-35.
29. Hoessel R, Leclerc S, Endicott JA, Nobel ME, Lawrie A, Tunnah P, et al. Indirubin, the active constituent of a Chinese antileukaemia medicine, inhibits cyclin-dependent kinases. *Nat Cell Biol* 1999;1(1):60-7.
30. Wu GY, Fang FD. [Studies on the mechanism of indirubin action in the treatment of chronic granulocytic leukemia. II. Effects of indirubin on nucleic acid and protein synthesis in animal transplantable tumor cells and normal proliferating cells in vitro (author's transl)]. *Zhongguo Yi Xue Ke Xue Yuan Xue Bao* 1980;2(2):83-7.
31. Meijer L, Skaltsounis AL, Magiatis P, Polychronopoulos P, Knockaert M, Leost M, et al. GSK-3-selective inhibitors derived from Tyrian purple indirubins. *Chem Biol* 2003;10(12):1255-66.
32. Leclerc S, Garnier M, Hoessel R, Marko D, Bibb JA, Snyder GL, et al. Indirubins inhibit glycogen synthase kinase-3 beta and CDK5/p25, two protein kinases involved in abnormal tau phosphorylation in Alzheimer's disease. A property common to most cyclin-dependent kinase inhibitors? *J Biol Chem* 2001;276(1):251-60.
33. Nam S, Buettner R, Turkson J, Kim D, Cheng JQ, Muehlbeyer S, et al. Indirubin derivatives inhibit Stat3 signaling and induce apoptosis in human cancer cells. *Proc Natl Acad Sci U S A* 2005;102(17):5998-6003.
34. De Landsheere BC. Effect of indirubin on white blood cell count of the guinea pig. *Experientia* 1951;7(8):307-8.
35. Ji XJ, Zhang FR, Lei JL, Xu YT. [Studies on the antineoplastic action and toxicity of synthetic indirubin (author's transl)]. *Yao Xue Xue Bao* 1981;16(2):146-8.

36. Wan JH, You YC, Mi JX, Ying HG. [Effect of indirubin on hemopoietic cell production (author's transl)]. *Zhongguo Yao Li Xue Bao* 1981;2(4):241-4.
37. Davies TG, Tunnah P, Meijer L, Marko D, Eisenbrand G, Endicott JA, et al. Inhibitor binding to active and inactive CDK2: the crystal structure of CDK2-cyclin A/indirubin-5-sulphonate. *Structure* 2001;9(5):389-97.
38. Ribas J, Bettayeb K, Ferandin Y, Knockaert M, Garrofe-Ochoa X, Totzke F, et al. 7-Bromoindirubin-3'-oxime induces caspase-independent cell death. *Oncogene* 2006;25(47):6304-18.
39. Ribas J, Yuste VJ, Garrofe-Ochoa X, Meijer L, Esquerda JE, Boix J. 7-Bromoindirubin-3'-oxime uncovers a serine protease-mediated paradigm of necrotic cell death. *Biochem Pharmacol* 2008;76(1):39-52.
40. Magiatis P, Polychronopoulos P, Skaltsounis AL, Lozach O, Meijer L, Miller DB, et al. Indirubins deplete striatal monoamines in the intact and MPTP-treated mouse brain and block kainate-induced striatal astrogliosis. *Neurotoxicol Teratol* 2010;32(2):212-9.
41. Wang FS, Ko JY, Weng LH, Yeh DW, Ke HJ, Wu SL. Inhibition of glycogen synthase kinase-3 β attenuates glucocorticoid-induced bone loss. *Life Sci* 2009;85(19-20):685-92.
42. Colletti M, Cicchini C, Conigliaro A, Santangelo L, Alonzi T, Pasquini E, et al. Convergence of Wnt signaling on the HNF4 α -driven transcription in controlling liver zonation. *Gastroenterology* 2009;137(2):660-72.
43. Vougianniopoulou K, Ferandin Y, Bettayeb K, Myriantopoulos V, Lozach O, Fan Y, et al. Soluble 3',6-substituted indirubins with enhanced selectivity toward glycogen synthase kinase -3 alter circadian period. *J Med Chem* 2008;51(20):6421-31.
44. Lluis F, Pedone E, Pepe S, Cosma MP. Periodic activation of Wnt/ β -catenin signaling enhances somatic cell reprogramming mediated by cell fusion. *Cell Stem Cell* 2008;3(5):493-507.
45. Sato N, Meijer L, Skaltsounis L, Greengard P, Brivanlou AH. Maintenance of pluripotency in human and mouse embryonic stem cells through activation of Wnt signaling by a pharmacological GSK-3-specific inhibitor. *Nat Med* 2004;10(1):55-63.
46. Ullmann U, Gilles C, De Rycke M, Van de Velde H, Sermon K, Liebaers I. GSK-3-specific inhibitor-supplemented hESC medium prevents the epithelial-

- mesenchymal transition process and the up-regulation of matrix metalloproteinases in hESCs cultured in feeder-free conditions. *Mol Hum Reprod* 2008;14(3):169-79.
47. Galmozzi E, Facchetti F, La Porta CA. Cancer stem cells and therapeutic perspectives. *Curr Med Chem* 2006;13(6):603-7.
 48. Horner MJ RL, Krapcho M, Neyman N, Aminou R, Howlader N, et al (eds). SEER Cancer Statistics Review, 1975-2006. National Cancer Institute. Bethesda, MD. 2009.
 49. Hortobagyi GN, de la Garza Salazar J, Pritchard K, Amadori D, Haidinger R, Hudis CA, et al. The global breast cancer burden: variations in epidemiology and survival. *Clin Breast Cancer* 2005;6(5):391-401.
 50. Gasent Blesa JM, Alberola Candel V, Esteban Gonzalez E, Vidal Martinez J, Gisbert Criado R, Provencio Pulla M, et al. Circulating tumor cells in breast cancer: methodology and clinical repercussions. *Clin Transl Oncol* 2008;10(7):399-406.
 51. Bogenrieder T, Herlyn M. Axis of evil: molecular mechanisms of cancer metastasis. *Oncogene* 2003;22(42):6524-36.
 52. Carlson RW. NCCN breast cancer clinical practice guidelines in oncology: an update. *J Natl Compr Canc Netw* 2003;1 Suppl 1:S61-3.
 53. Swanton C, Szallasi Z, Brenton JD, Downward J. Functional genomic analysis of drug sensitivity pathways to guide adjuvant strategies in breast cancer. *Breast Cancer Res* 2008;10(5):214.
 54. Magne N, Chargari C, Conforti R, Toillon RA, Bauduceau O, Vedrine L, et al. [Mechanisms of resistance to molecular targeted therapies in breast cancer: update and future]. *Bull Cancer* 2010;97(3):385-95.
 55. Castrellon AB, Gluck S. Chemoprevention of breast cancer. *Expert Rev Anticancer Ther* 2008;8(3):443-52.
 56. Gupta GP, Massague J. Cancer metastasis: building a framework. *Cell* 2006;127(4):679-95.
 57. Shiozawa Y, Havens AM, Pienta KJ, Taichman RS. The bone marrow niche: habitat to hematopoietic and mesenchymal stem cells, and unwitting host to molecular parasites. *Leukemia* 2008;22(5):941-50.
 58. Wehrle-Haller B, Imhof BA. Actin, microtubules and focal adhesion dynamics during cell migration. *Int J Biochem Cell Biol* 2003;35(1):39-50.

59. Pollard TD, Borisy GG. Cellular motility driven by assembly and disassembly of actin filaments. *Cell* 2003;112(4):453-65.
60. DeMali KA, Wennerberg K, Burridge K. Integrin signaling to the actin cytoskeleton. *Curr Opin Cell Biol* 2003;15(5):572-82.
61. Hannigan G, Troussard AA, Dedhar S. Integrin-linked kinase: a cancer therapeutic target unique among its ILK. *Nat Rev Cancer* 2005;5(1):51-63.
62. Desgrosellier JS, Cheresch DA. Integrins in cancer: biological implications and therapeutic opportunities. *Nat Rev Cancer* 2010;10(1):9-22.
63. Allingham JS, Klenchin VA, Rayment I. Actin-targeting natural products: structures, properties and mechanisms of action. *Cell Mol Life Sci* 2006;63(18):2119-34.
64. Jiang P, Enomoto A, Takahashi M. Cell biology of the movement of breast cancer cells: intracellular signalling and the actin cytoskeleton. *Cancer Lett* 2009;284(2):122-30.
65. Caswell PT, Vadrevu S, Norman JC. Integrins: masters and slaves of endocytic transport. *Nat Rev Mol Cell Biol* 2009;10(12):843-53.
66. Guo W, Giancotti FG. Integrin signalling during tumour progression. *Nat Rev Mol Cell Biol* 2004;5(10):816-26.
67. Somanath PR, Kandel ES, Hay N, Byzova TV. Akt1 signaling regulates integrin activation, matrix recognition, and fibronectin assembly. *J Biol Chem* 2007;282(31):22964-76.
68. Kim D, Chung J. Akt: versatile mediator of cell survival and beyond. *J Biochem Mol Biol* 2002;35(1):106-15.
69. Wang J, Wan W, Sun R, Liu Y, Sun X, Ma D, et al. Reduction of Akt2 expression inhibits chemotaxis signal transduction in human breast cancer cells. *Cell Signal* 2008;20(6):1025-34.
70. Mora A, Komander D, van Aalten DM, Alessi DR. PDK1, the master regulator of AGC kinase signal transduction. *Semin Cell Dev Biol* 2004;15(2):161-70.
71. Sarbassov DD, Guertin DA, Ali SM, Sabatini DM. Phosphorylation and regulation of Akt/PKB by the rictor-mTOR complex. *Science* 2005;307(5712):1098-101.
72. Du K, Tsichlis PN. Regulation of the Akt kinase by interacting proteins. *Oncogene* 2005;24(50):7401-9.

73. Chan TO, Tsihchlis PN. PDK2: a complex tail in one Akt. *Sci STKE* 2001;2001(66):pe1.
74. Dong LQ, Liu F. PDK2: the missing piece in the receptor tyrosine kinase signaling pathway puzzle. *Am J Physiol Endocrinol Metab* 2005;289(2):E187-96.
75. Grille SJ, Bellacosa A, Upson J, Klein-Szanto AJ, van Roy F, Lee-Kwon W, et al. The protein kinase Akt induces epithelial mesenchymal transition and promotes enhanced motility and invasiveness of squamous cell carcinoma lines. *Cancer Res* 2003;63(9):2172-8.
76. Roberts MS, Woods AJ, Dale TC, Van Der Sluijs P, Norman JC. Protein kinase B/Akt acts via glycogen synthase kinase 3 to regulate recycling of alpha v beta 3 and alpha 5 beta 1 integrins. *Mol Cell Biol* 2004;24(4):1505-15.
77. Somanath PR, Chen J, Byzova TV. Akt1 is necessary for the vascular maturation and angiogenesis during cutaneous wound healing. *Angiogenesis* 2008;11(3):277-88.
78. Hynes RO. Integrins: bidirectional, allosteric signaling machines. *Cell* 2002;110(6):673-87.
79. Vicente-Manzanares M, Choi CK, Horwitz AR. Integrins in cell migration--the actin connection. *J Cell Sci* 2009;122(Pt 2):199-206.
80. Ridley AJ, Schwartz MA, Burridge K, Firtel RA, Ginsberg MH, Borisy G, et al. Cell migration: integrating signals from front to back. *Science* 2003;302(5651):1704-9.
81. Lee JW, Juliano RL. The alpha5beta1 integrin selectively enhances epidermal growth factor signaling to the phosphatidylinositol-3-kinase/Akt pathway in intestinal epithelial cells. *Biochim Biophys Acta* 2002;1542(1-3):23-31.
82. Caswell PT, Chan M, Lindsay AJ, McCaffrey MW, Boettiger D, Norman JC. Rab-coupling protein coordinates recycling of alpha5beta1 integrin and EGFR1 to promote cell migration in 3D microenvironments. *J Cell Biol* 2008;183(1):143-55.
83. Li J, Ballif BA, Powelka AM, Dai J, Gygi SP, Hsu VW. Phosphorylation of ACAP1 by Akt regulates the stimulation-dependent recycling of integrin beta1 to control cell migration. *Dev Cell* 2005;9(5):663-73.
84. Mulrooney JP, Hong T, Grabel LB. Serine 785 phosphorylation of the beta1 cytoplasmic domain modulates beta1A-integrin-dependent functions. *J Cell Sci* 2001;114(Pt 13):2525-33.

85. Nicoletti I, Migliorati G, Pagliacci MC, Grignani F, Riccardi C. A rapid and simple method for measuring thymocyte apoptosis by propidium iodide staining and flow cytometry. *J Immunol Methods* 1991;139(2):271-9.
86. Bourguignon LY, Zhu H, Shao L, Chen YW. CD44 interaction with c-Src kinase promotes cortactin-mediated cytoskeleton function and hyaluronic acid-dependent ovarian tumor cell migration. *J Biol Chem* 2001;276(10):7327-36.
87. Bradford MM. A rapid and sensitive method for the quantitation of microgram quantities of protein utilizing the principle of protein-dye binding. *Anal Biochem* 1976;72:248-54.
88. Laemmli UK. Cleavage of structural proteins during the assembly of the head of bacteriophage T4. *Nature* 1970;227(5259):680-5.
89. Lin RZ, Chang HY. Recent advances in three-dimensional multicellular spheroid culture for biomedical research. *Biotechnol J* 2008;3(9-10):1172-84.
90. Takagi J, Strokovich K, Springer TA, Walz T. Structure of integrin alpha5beta1 in complex with fibronectin. *EMBO J* 2003;22(18):4607-15.
91. Kotha J, Longhurst C, Appling W, Jennings LK. Tetraspanin CD9 regulates beta 1 integrin activation and enhances cell motility to fibronectin via a PI-3 kinase-dependent pathway. *Exp Cell Res* 2008;314(8):1811-22.
92. Parsons JT, Martin KH, Slack JK, Taylor JM, Weed SA. Focal adhesion kinase: a regulator of focal adhesion dynamics and cell movement. *Oncogene* 2000;19(49):5606-13.
93. Ridley AJ. Rho GTPases and cell migration. *J Cell Sci* 2001;114(Pt 15):2713-22.
94. Westhoff MA, Fulda S. Adhesion-mediated apoptosis resistance in cancer. *Drug Resist Updat* 2009;12(4-5):127-36.
95. Mitchison TJ, Cramer LP. Actin-based cell motility and cell locomotion. *Cell* 1996;84(3):371-9.
96. Dancey J, Sausville EA. Issues and progress with protein kinase inhibitors for cancer treatment. *Nat Rev Drug Discov* 2003;2(4):296-313.
97. Tkaczuk KH. Review of the contemporary cytotoxic and biologic combinations available for the treatment of metastatic breast cancer. *Clin Ther* 2009;31 Pt 2:2273-89.

98. Danen EH. Integrins: regulators of tissue function and cancer progression. *Curr Pharm Des* 2005;11(7):881-91.
99. Bretscher MS. Moving membrane up to the front of migrating cells. *Cell* 1996;85(4):465-7.
100. Chen HC, Appeddu PA, Isoda H, Guan JL. Phosphorylation of tyrosine 397 in focal adhesion kinase is required for binding phosphatidylinositol 3-kinase. *J Biol Chem* 1996;271(42):26329-34.
101. Lurje G, Lenz HJ. EGFR signaling and drug discovery. *Oncology* 2009;77(6):400-10.
102. Nishita M, Wang Y, Tomizawa C, Suzuki A, Niwa R, Uemura T, et al. Phosphoinositide 3-kinase-mediated activation of cofilin phosphatase Slingshot and its role for insulin-induced membrane protrusion. *J Biol Chem* 2004;279(8):7193-8.
103. Mazzoleni G, Di Lorenzo D, Steimberg N. Modelling tissues in 3D: the next future of pharmaco-toxicology and food research? *Genes Nutr* 2009;4(1):13-22.
104. Mayer B, Klement G, Kaneko M, Man S, Jothy S, Rak J, et al. Multicellular gastric cancer spheroids recapitulate growth pattern and differentiation phenotype of human gastric carcinomas. *Gastroenterology* 2001;121(4):839-52.
105. Chung CY, Funamoto S, Firtel RA. Signaling pathways controlling cell polarity and chemotaxis. *Trends Biochem Sci* 2001;26(9):557-66.

8 APPENDIX

8.1 Publications

8.1.1 Original publications

Pettit RK, Fakoury BR, Knight JC, **Weber CA[§]**, Pettit GR, Cage GD, Pon S. Antibacterial activity of the marine sponge constituent cribrostatin 6, JMM. 2004: 53: 61-65.

Pettit RK, **Weber CA[§]**, Kean MJ, Hoffmann H, Pettit GR, Tan R, Franks KS, Horton ML. Microplate Alamar blue assay for *Staphylococcus epidermidis* biofilm susceptibility testing. AAC. 2005: 49: 2612-2617.

Pettit GR, Tan R, Pettit RK, Smith T, Feng S, Doubek K biofilms. J Med Microbiol. 2009: 58: 1203-6.

Pettit RK, **Weber CA[§]**, Pettit GR. Application of a high throughput Alamar blue biofilm susceptibility assay to *Staphylococcus aureus* biofilms. Ann Clin Microbiol Antimicrob. 2009: 8(1): 28.

Pettit RK, Pettit GR, Xu JP, **Weber CA[§]**, Richert L. Isolation of human cancer cell growth inhibitory, antimicrobial lateritin from a mixed fungal culture. Pla Medica. 2010: 76(5): 500-1.

§ Maiden name,

Married name: Kressirer

8.1.2 Poster presentations

Weber CA[§], RK Pettit, GR Pettit. Microplate Alamar blue assay for *Staphylococcus epidermidis* biofilm susceptibility testing, at the International Union of Microbiological Sciences, San Francisco, California, July 2005.

Weber CA[§], Meijer L, Vollmar AK. Induction of apoptosis and inhibition of proliferation and migration of human tumor cells by an indirubin derivative, at the 51. Jahrestagung der Deutschen Gesellschaft für Experimentelle und Klinische Pharmakologie und Toxikologie (DGPT), Mainz, Germany, March 2010.

§ Maiden name,

Married name: Kressirer

8.2 Grants and awards

March 2010

DGPT Travel Grant

Convention Travel to the 51. Jahrestagung der Deutschen Gesellschaft für Experimentelle und Klinische Pharmakologie und Toxikologie (DGPT), Mainz, Germany.

January 2007 - 2010

Stipendium (Full Study Scholarship)

Bayerische Forschungstiftung, Munich, Germany

8.3 Curriculum Vitae

Personal Data

Name	Christine Ann Kressirer, geb. Weber
Date of Birth	January 9th, 1980
Place of Birth	Milwaukee, WI USA
Nationality	American

Academic Education

January 2007 - July 2010	PhD Thesis Department of Pharmaceutical Biology Chair: Prof. Dr. Angelika M. Vollmar Ludwig-Maximilians-University, Munich, Germany
August 1998 - May 2002	Bachelor of Science Microbiology College of Veterinary Medicine/ Biomedical Sciences Colorado State University, Fort Collins, CO USA
August 1998 - May 2002	Bachelor of Arts Biochemistry Department of Biochemistry and Molecular Biology Colorado State University, Fort Collins, CO USA

Laboratory Experience

2006-2007	Laboratory Coordinator School of Life Sciences Arizona State University Tempe, AZ USA
2002-2006	Research Specialist Cancer Research Institute Arizona State University Tempe, AZ USA
1998-2001	Student Lab Tech II Department of Biochemistry and Molecular Biology Colorado State University, Fort Collins, CO USA

8.4 Acknowledgments

First and foremost, I offer my sincerest gratitude to my family and friends in America for their constant loving support and encouragement. The discussions about my project, the phone calls, the late night Skype sessions and endless emails gave me encouragement or just a smile when I needed them the most.

Living and studying abroad has exposed me to many experiences that I would have otherwise missed in my life. I am indebted to many of my colleagues and LMU groups for their support in the lab and the attempts to integrate me into the German, moreover the Bavarian society. To the new friends and colleagues, who are scattered around the world, what can I say? I am blessed to have been exposed to your cultures and will not forget the crazy food items, the random words taught and learned and the sometimes very (VERY) different cultural norms.

A heartfelt thanks to my supervisor, Prof. Dr. Angelika Vollmar, whose knowledge and foresight has supported me through both the positive and negative results that every student faces during research. I appreciate her support of my ideas and the creative suggestions of her own, without them my thesis would not have been completed. I would also like to express my sincere gratitude to my second examiner, Prof. Dr. Marianne Jochum. She devoted considerable time and effort in improving this manuscript. I also appreciate the time and interest from Prof. Dr. Winter, Prof. Dr. Wahl, PD Dr. Ogris and Prof. Dr. Wanner, all of whom served as members of my thesis committee.

To the three apoptosis postdoctoral supervisors, Dr. Karin von Schwarzenberg Dr. Nichole Barth and Dr. Anita Rudy, whose attention to my project is highly appreciated. A special thanks to PD Dr. Zahler, Dr. Culmsee and Prof. Dr. Wagner for their suggestions throughout various phases of my project. Without the gentle nudge from both Dr. Robin K. Pettit and Dr. George R. Pettit, I never would have decided to pursue my PhD: Thank you both for directing me to new opportunities.

Finally, I would like to thank my new family here in Bavaria for their loving support and patience. To my husband Martin: There are no words to express how much your love and consideration has helped me.